

38560

**RELATIONSHIPS BETWEEN THE PLASMA SPRAYING PARAMETERS AND
QUALITY OF Co-Mo-Cr-Si COATINGS**

A THESIS SUBMITTED TO
THE GRADUATE SCHOOL OF NATURAL AND APPLIED SCIENCES
OF
THE MIDDLE EAST TECHNICAL UNIVERSITY

BY

İHSAN GÜLER

IN PARTIAL FULFILLMENT OF THE REQUIREMENTS FOR THE DEGREE
OF MASTER OF SCIENCE

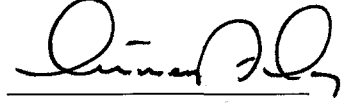
IN

THE DEPARTMENT OF METALLURGICAL ENGINEERING

APRIL 1995

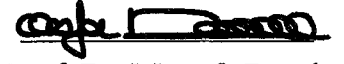
**T.C. YÜKSEKÖĞRETİM KURULU
DOKÜMANTASYON MERKEZİ**

Approval of the Graduate School of Natural and Applied Sciences



Prof. Dr. İsmail Tosun
for Director

I certify that this thesis satisfies all the requirements as a thesis for the degree of Master of Science.



Prof. Dr. Mustafa Doruk
Head of Department

This is to certify that we have read this thesis and that in our opinion it is fully adequate, in scope and quality, as a thesis for the degree of Master of Science.



Prof. Dr. Mustafa Doruk
Supervisor

Examining Committee Members

Prof. Dr. Ordal Demokan



Prof. Dr. Mustafa Doruk



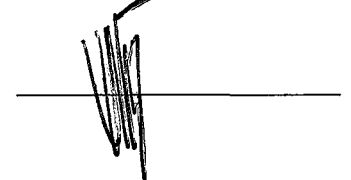
Yard. Doç. Dr. Ali Kalkanlı



Yard. Doç. Dr. Bilgehan Ögel



Yard. Doç. Dr. Vedat Akdeniz



ABSTRACT

RELATIONSHIPS BETWEEN THE PLASMA SPRAYING PARAMETERS AND QUALITY OF THE Co-Mo-Cr-Si COATINGS

GÜLER, İhsan

M.S. , Metallurgical Engineering

Supervisor: Prof. Dr. Mustafa DORUK

April 1995, 69 pages.

In this study, the effects of several plasma spraying parameters on the coating quality were investigated. To analyze these effects, numerous tests having different spraying parameters were done. The evaluation of these tests were according to change in the microstructures and the mechanical properties of the coatings. As a result of this study, it was found that the electric input, spraying distance and the amount of powder fed into the torch are primary parameters. Furthermore, the traverse speed of the torch and air cooling of the substrate during spraying are determined to be the secondary parameters that affect the quality of the coating.

Keywords: Plasma, Plasma Beam, Plasma Spraying, Plasma Spraying Parameters.

ÖZ

Co-Mo-Cr-Si KAPLAMALARININ KALİTESİNİN PLAZMA PÜSKÜRTME PARAMETRELERİYLE İLİŞKİSİ

GÜLER, İhsan

Yüksek Lisans Tezi, Metalurji Mühendisliği Anabilim Dalı

Tez Yöneticisi: Prof. Dr. Mustafa DORUK

Nisan, 1995, 69 sayfa

Bu çalışmada, kaplama kalitesinde etkili olan birçok plazma püskürtme parametresi incelendi. Bu etkileri analiz ederken birçok farklı parametrelerde testler yapıldı. Bu testler kaplamaların mikroyapı ve mekanik özelliklerindeki değişimlerine göre değerlendirildi. Bu çalışmanın sonucunda elektrik gücü, püskürtme mesafesi ve tabancaya verilen toz miktarının birincil parametreler olduğu bulundu. Bundan başka, tabanca hızı ve püskürtme sırasında asıl malzemenin soğutulmasında kaplama kalitesini etkileyen ikincil parametreler olduğu saptandı.

Anahtar Kelimeler: Plazma, Plazma Işını, Plazma Püskürtme, Plazma Püskürtme Parametreleri.



To my Parents

ACKNOWLEDGEMENTS

First I would like to express my great appreciation to Prof. Dr. Mustafa Doruk for his valuable support and constant guidance. I must also express my gratitude to Mr. Nadi Köklü, General Manager, Mr. Tayfun Mutlu, Plant Manager and Mr. Nadir Şen, Director of Assembly Department of Tusaş Engine Industries. Also I would like to thank to the personnel who have given me their valuable helps in the Quality Control and Special Process Departments.



TABLE OF CONTENTS

ABSTRACT	iii
ÖZ	iv
ACKNOWLEDGEMENTS	vi
TABLE OF CONTENTS	vii
LIST OF TABLES	x
LIST OF FIGURES	xi
CHAPTER	
1. INTRODUCTION	1
2. PRINCIPLES OF PLASMA SPRAYING PROCESS	3
2.1 Plasma Beam	3
2.1.1 Temperature and Output of Plasma Beam.....	7
2.1.2 Outlet Velocity:.....	8
2.2 Plasma Gases.....	9
2.3 Formation of Plasma Coatings	10
2.3.1 Powder Transport, Flight Path and Velocity of the Sprayed Particles	10
2.3.2 Interactions of Molten Material with the Plasma Beam and the Surrounding Atmosphere	12
2.3.3 Impingement of Flying Particles on the Substrate.....	13
2.3.4 Thermal Effects of the Substrate and the Sprayed Layer.....	14

2.3.5	Physical and Chemical Transformation of Material in Spraying.....	14
2.4	Basic Properties of Plasma Sprayed Coatings.....	15
2.4.1	Structure.....	16
2.4.2	Density and Porosity.....	16
2.4.3	Bonding, Internal Stresses.....	17
2.4.4	Strength, Hardness.....	18
2.5	Bonding and Adherence of Plasma Coatings to the Substrate.....	18
2.5.1	Kinds of Bonding Forces.....	18
2.5.2	Metallographic Analysis of the Bond.....	20
3.	EXPERIMENTAL SETUP AND PROCEDURE.....	23
3.1	Plasma Spraying Equipment.....	23
3.1.1	Metco 9M Plasma Spray System.....	23
3.2	Procedure of Plasma Spraying.....	26
3.2.1	Preliminary Preparation of Surfaces Prior to Spraying..	26
3.2.2	Chemical Degreasing.....	27
3.2.3	Abrasive Cleaning.....	27
3.2.4	Application of Interlayers Improving Adherence.....	27
3.2.5	Working Parameters of the Spraying Process.....	28
3.3	Materials.....	29
3.4	Test Specimens.....	30
3.5	Tensile Bond Strength Test.....	30
3.6	Hardness Measurements.....	31
3.7	Evaluation of the Microstructure of the Coatings.....	31
3.8	Experimental Program.....	32

4. RESULTS AND DISCUSSION	37
4.1 Effect of the Primary Plasma Spraying Parameters on the Properties of the Coating.....	40
4.1.1 Effect of Distance.....	40
4.1.2 Effect of Electric Input and Gas Flow Rate.....	43
4.1.3 Effect of Spray Rate and Carrier Flow Rate.....	48
4.1.4 Effect of Preheat	54
4.1.5 Effect of Interlayer	57
4.2 Effect of Secondary Plasma Spraying Parameters.....	59
5. CONCLUSIONS	61
REFERENCES.....	63
APPENDIX	
TEST PROCEDURE TO IMPROVE THE COATING QUALITY OF AN AIRCRAFT ENGINE PART OF TEI.....	65

LIST OF TABLES

TABLE

2.1	The contents of O ₂ and N ₂ in the layers of the sprayed materials.....	15
3.1	Test parameters	34
3.2	Change in Electric Input	35
3.3	Effect of Spray Rate	35
3.4	Effect of Spraying Distance.....	35
3.5	Plasma Spraying Parameters of the interlayer type B50TF56 Cl- A.....	36
4.1	Hardness Results (with bond coat).....	37
4.2	Hardness Results (with bond coat)	37
4.3	Hardness Results (with bond coat)	38
4.4	Hardness Results.....	38
4.5	Tensile Test Results.....	39
4.6	Microstructural Test Results (Optical Microscope 200×)	39

LIST OF FIGURES

FIGURES

2.1	Excitation of a neutral atom	4
2.2	Plasma Torch with non- transferred arc.....	6
2.3	Plasma Torch with transferred arc.....	6
2.4	Distribution of temperatures in plasma beam	7
2.5	Inclination of beam of molten particles.....	11
2.6	Particle deformation on the substrate.....	13
2.7	Types of coating bonds with substrate.....	20
2.8	Coating structure	21
4.1	Effect of spraying distance on hardness and tensile strength.....	40
4.2	Comparing the effects of the spraying distance on hardness of the coatings with and without bondcoat.	41
4.3	Microstructure of the coat, sprayed at 3 inches (200×).	41
4.4	Microstructure of the coat, sprayed at 4 inches (200×)	42
4.5	Microstructure of the coat, sprayed at 5 inches (200×)	43
4.6	Effect of electric input on tensile strength and hardness of the coating.	44
4.7	Total effect of primary and secondary gas flow rates on tensile strength and hardness of the coating.	45

4.8	Microstructure of the coat, sprayed at 124 scfh gas flow rate (200×).	46
4.9	Microstructure of the coat, sprayed at 140 scfh gas flow rate (200×).	47
4.10	Microstructure of the coat, sprayed at 150 scfh gas flow rate (200×).	47
4.11	Microstructure of the coat, sprayed at 160 scfh gas flow rate (200×).	48
4.12	With lowering the inlet velocity of the powders, h angle increases.	49
4.13	Microstructure of the coat, sprayed at 7 scfh and 45 gr/min (200×).	50
4.14	Microstructure of the coat, sprayed at 11 scfh and 60 gr/min (200×).	50
4.15	Microstructure of the coat, sprayed at 15 scfh and 45 gr/min (200×).	51
4.16	Microstructure of the coat, sprayed at 11 scfh and 30 gr/min (200×).	52
4.17	Effect of carrier gas flow, at a constant spray rate of 45 gr/min, on the tensile strength and hardness of the coatings.	52
4.18	Effect of spray rate, at a constant carrier flow of 11 scfh.	53
4.19	Combined effects of spray rate and carrier gas flow, on the tensile strength and hardness of the coatings.	53
4.20	Effect of number of preheat passes of the torch on the tensile strength and hardness of the coatings.	54
4.21	Microstructure of the coat, sprayed after two preheating passes (200×).	55
4.22	Microstructure of the coat, sprayed after four preheating passes (200×).	55
4.23	Microstructure of the coat, sprayed on the nonpreheated test coupon (200×).	57
4.24	Effect of bond coat with different spraying parameters.	58
4.25	Effect of bond coat with different spraying parameters.	58

CHAPTER 1

INTRODUCTION

Plasma Spraying Technology is employed in many diverse areas in industry and research. The reason of its utilization is to achieve desired properties, such as: abrasive wear resistance, fatigue resistance, erosive wear resistance, resistance against high temperature oxidation, corrosion resistance on the surface of the parts. It is also used in the renovation of worn parts. The major advantage of this among the other spraying techniques is the widest range of materials can be sprayed.

This process is extensively used in aircraft industry for the production of aircraft jet engines. The working parts of aircraft jet engines are subjected to severe mechanical, chemical and thermal stresses. A jet engine has a number of construction nodes where plasma coatings are applied with success from room temperature up to high temperatures [1- 5]. The face of the blower box, compressor bosses and discs, guide bearings, fuel nozzles, blades of the low pressure and high pressure compressor, combustion chambers and adjacent boxes, seal linings of rotary and stationary parts of compressor and turbine etc., are plasma sprayed to achieve several properties. The sprayed coatings protect these parts against wear and high temperature effects, they form abrasive and abradable seal layers and they protect against high temperature corrosion.

The coating parameters can be divided into two categories according to their effect on the coating quality: primary and secondary parameters.

In the case of primary parameters, basic spraying requirements are provided to form an optimum coating structure. These are, heat input to melt

powders, flight path of powders during spraying, and conditions of substrate that affects bonding with molten powders.

In some cases, the primary parameters are used, but required coating structure may not be achieved. Generally, this is due to improper control of secondary parameters. In addition to this fact, they can cause excessive deterioration of the coating microstructure. A study was done on an aircraft engine part to show the effects of secondary parameters, that are mostly undetermined and ignored [4]. As concluded from this study, if it is desired to achieve optimum coating quality, that will never be disturbed even after thousands of sprayings, both of the effects of primary and secondary spraying parameters should be mutually considered.

The present study was undertaken to shed further light on the relationships between plasma spraying parameters and the coating quality whereby a special attention was paid to underlying mechanisms.

CHAPTER 2

PRINCIPLES OF PLASMA SPRAYING PROCESS

2.1 Plasma Beam

For better understanding of the term 'plasma beam' some explanation of principles from the theory of gas mechanics would be helpful. The properties of the gas are primarily dependent upon the movement of its individual molecules. During this movement, the molecules cooperatively exchange the energy and pulse due to collisions of their elementary particles. If a certain amount of energy is supplied to a gas, the velocity of the molecules increases. The higher this velocity, the more frequent are the mutual collisions of the particles. A temperature increase of the affected gas is thus a natural consequence of this energy process. The velocity of the particles may attain such a high level that, in the case of a two atom gas, the molecules disintegrate into atoms due to mutual collisions. This process, taking place in the plasma arc, is called dissociation. In the case of hydrogen molecules, the dissociation process takes place within the 2500-6000 K temperature range. When higher levels of energy are supplied, the velocity can achieve such a high level that not only molecules dissociated, but also electrons can be forced out from the electron cover of atoms. The energy needed for forcing an electron from its path is higher than the energy needed for the dissociation process and it is called the ionization energy, and the whole process, taking place also in the plasma arc, is called ionization.

The ionization process can be explained in more detail with the example of an atom with two electrons (Fig. 2.1). Around the atom nucleus with two + charges,

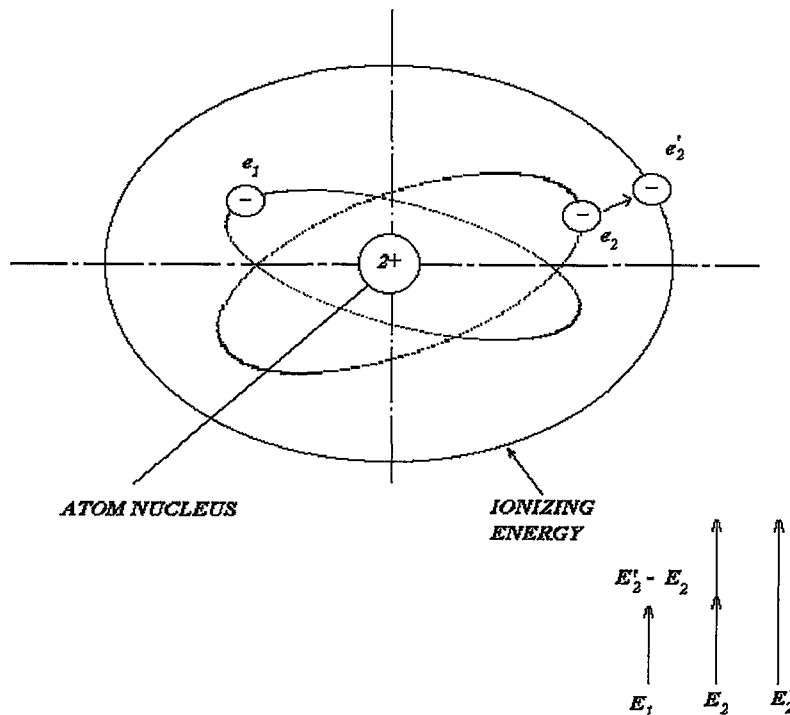


Figure 2.1 Excitation of a neutral atom

two electrons, e_1 and e_2 rotate in two paths close to the nucleus. Each electron has its own energy, E_1 , E_2 . The normal condition of this atom is neutral, since both $+$ charges of the nucleus are balanced with the two $-$ charges of electrons that rotate around the nucleus. When sufficient energy is supplied from outside at least one electron e_2 , the one with the highest energy E_2 will jump over to the next orbit, characterized by a higher energy E_2' . The atom is now in the excited state. The amount of energy necessary for forcing the electron from its original position, to ionize the atom, is called the ionization energy of that atom. At this stage, two particles can already be distinguished. The first one is the ionized atom- the original atom without one electron- and the other is the free electron. The ionized atom is called an ion, while its electric charge without one electron is $+1$. The free electron has a $-$ charge.

The final consequence of the whole dissociation and ionization processes is plasma as a state of mass, containing the electrically charged particles. However, it must be noted that the plasma is apparently neutral, since in it, the same number of electrically positive and negative charges must be distributed. The processes of dissociation and ionization are thermally balanced. This means that in dependence on

temperature, an equilibrium state between dissociation and ionization on the other hand, is attained [6].

To start ionization, the action of an external force is necessary, so that heavy collisions of particle occur. This external force can either be the action of high temperature or the action of an electric HF field. Depending on the kind of external force, the thermal (arc) or high frequency plasmas can be distinguished. The study was made by using the thermal plasma as the source of high temperature [7].

The technical creation and utilization of plasma as the high temperature source is realized in the plasma torch, also known as the plasma gun. Depending on the arrangement of the electrodes between which the electric plasma arc burns, two basic types of plasma torches can be distinguished. When the arc burns between the negative cathode and positive anode, realized as a nozzle inside the torch, it is classified as a torch with a non-transferred arc (Fig. 2.2).

When the positive pole from the nozzle is transferred to an external conductive material located in front of the nozzle, the arc will burn between the cathode inside the torch and the external conductor. In such a case it is classified as a torch with a transferred plasma arc (Fig. 2.3) [7]. In non-transferred arc torch the electric arc is ignited between the tungsten cathode and a copper anode in the form of a nozzle [2]. The plasma gas entering the nozzle is heated by the electric arc energy to a high temperature, causing the dissociation of two atom gases and the dissociation and partial ionization of one atom gases. Through the dissociation and ionization processes, the plasma gas transfers into a plasma state, and a large volume of thermal and kinetic energy is released, in the form of a plasma beam, and leaves the nozzle.

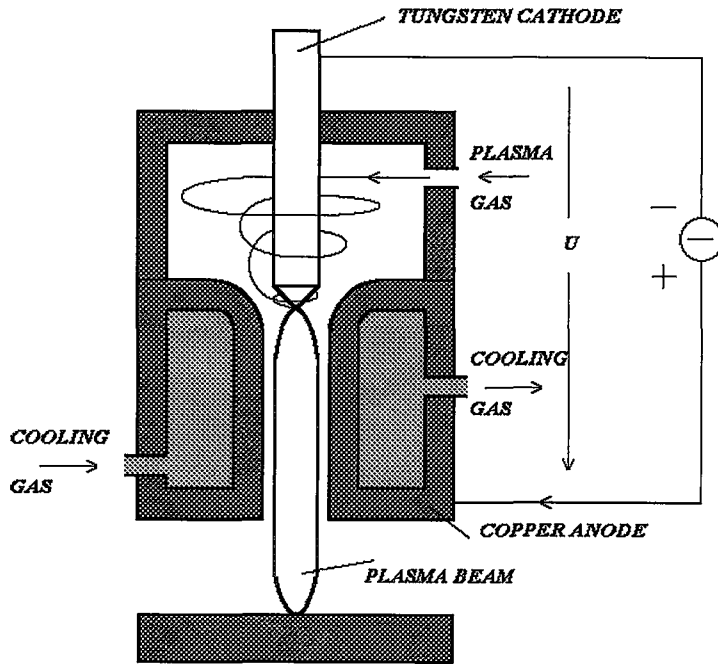


Figure 2.2 Plasma Torch with non- transferred arc

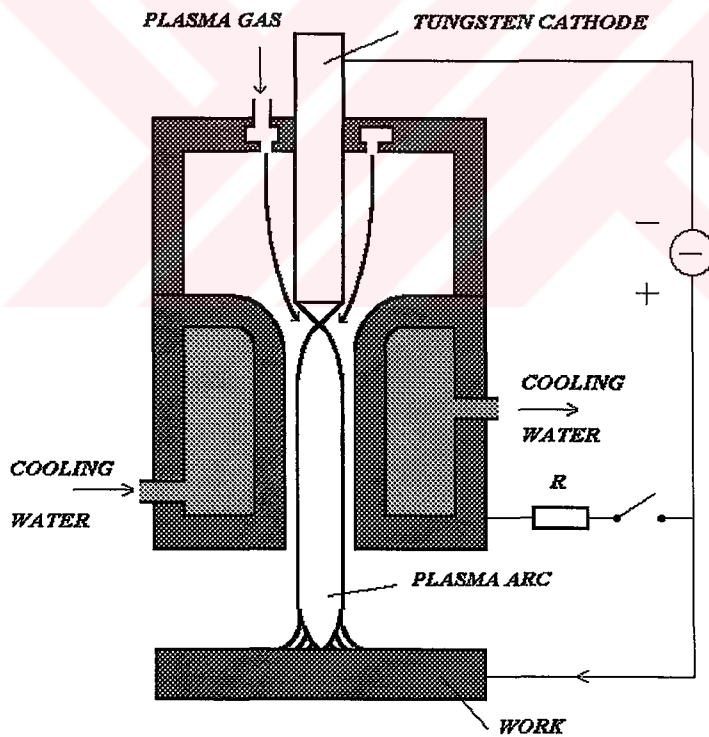


Figure 2.3 Plasma Torch with transferred arc

The temperature in the plasma arc center even attains 30,000 K and the outlet velocity of the plasma beam jetting from the nozzle is supersonic [5].

2.1.1 Temperature and Output of Plasma Beam

The output, temperature and velocity are the main characteristics of a plasma beam. The temperature of a plasma beam depends mainly on the ionization degree, that is affected by the kind of plasma gas and the working parameters of the plasma torch. A typical temperature distribution in a plasma beam is shown in Fig. 2.4. Plasma temperatures in this case reach 5000 to 30,000 K. Fig. 2.4a shows the temperature distribution in a laminar argon plasma beam (gas flow rate 4.5 l/min., 6 mm nozzle diameter) and that in turbulent argon beam is shown in Fig. 2.4b [5]. Very long isotherms of laminar flow suggest that no turbulent mixing of surrounding air with the hot gas beam occurs. This observation is obviously not valid for the turbulent flow whose isotherms are very short. Local temperature in a plasma beam is measured by means of spectroscopy. However, precise determination of temperature is rather questionable because of absorption of radiation by the hardly transparent plasma beam, and because of abrupt temperature deviations.

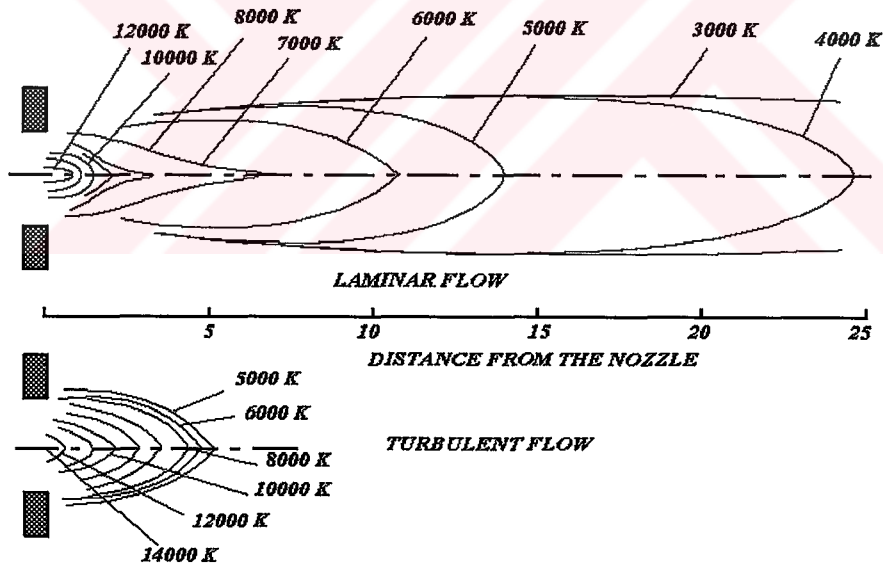


Figure 2.4 Distribution of temperatures in plasma beam

2.1.2 Outlet Velocity:

The velocity of a plasma beam can be calculated approximately by applying the fundamental gas mechanics laws to the condition of a gas flow through a cylindrical tube, during its simultaneous heating. With a lowered density in the flow direction during heating, the flow velocity increases. The dependence of velocity before and after heating can be obtained from the equation of a constant flow rate (flow rate equation) [8].

$$\rho_0 \cdot v_0 = \rho \cdot v \quad (1)$$

and from the state equation of the gas:

$$\frac{p_0}{\rho_0} \cdot T = \frac{P}{\rho} \cdot T_0 \quad (2)$$

where, ρ_0 and ρ are the gas densities at the inlet and outlet from the nozzle,
 p_0 and P are the pressures at the inlet and outlet from the nozzle (or cold and heated gas),
 T_0 and T are the temperatures of cold and heated gas in K, determined from the enthalpy,
 v_0 and v are the flow velocities at the inlet and outlet from the nozzle.

Provided that the gas pressure remains constant while the gas is heated it will be valid that

$$\frac{v_0}{T_0} = \frac{v}{T} \quad (3)$$

and

$$v = v_0 \cdot \frac{T}{T_0} \quad (4)$$

The velocity of plasma beam can also be calculated in terms of the plasma beam output, gas volume and its properties and on the nozzle diameter according the relationship [9]

$$v = A \cdot \frac{Q_0}{d^2} \cdot \frac{T}{M} \quad (5)$$

where, v - plasma beam velocity ($\text{m} \cdot \text{s}^{-1}$),
 Q_0 - volume of gas flow rate ($\text{m}^3 \cdot \text{s}^{-1}$),
 T - gas temperature (K),
 d - nozzle diameter (m),
 A - constant, and
 M - molecular weight of gas.

Considering equation (5) it can be concluded that the plasma beam velocity is directly proportional to the gas flow rate and indirectly proportional to the square of nozzle diameter.

Plasma beam velocity is considerably affected by any increase in the flow rate of the carrying gas which besides causing hydrostatic effects, also decreases the plasma temperature and velocity. The design of modern plasma torches is aimed at achieving the highest possible velocities, exceeding the velocity of sound. Such high velocities of the plasma beam, together with its high temperature, ensure a high rate of heat transfer on the filler material predetermined for melting and spraying, what provides the molten particles with high kinetic energy which favorably affects the quality of the layer formed at impingements of the flying molten particles on the substrate [1].

2.2 Plasma Gases

At present, mainly the gases such as Ar, He, N₂, H₂ and to a less extent also air and water (torches with water stabilization), are brought into the plasma state. The plasma forming gases are divided into two basic groups- one atom and two atom

gases. Argon and helium belong to the first group, while nitrogen and hydrogen belong to the other. The task of the gaseous environment in the plasma torch consists first of all in plasma formation and also protection of the electrodes against oxidation and their cooling. The plasma forming gas is selected on the basis of the desired temperature and velocity of the plasma beam and the degree of inertness in the sprayed material and substrate [2].

2.3 Formation of Plasma Coatings

The process of plasma coating formation consists of several stages that affect the properties of sprayed layer. Mainly the high thermal and kinetic energy of the plasma beam enables the melting and acceleration of the particles of the supplied powder. The methods of powder transport to the plasma torch, together with the shape and granularity of powder, then affect the formation of the paths of particles at a certain velocity. Interaction of the molten material with the plasma beam and the surrounding atmosphere affects the way the particles in the plasma beam melt and transforms physically and chemically. The mechanical, chemical and thermal conditions at the impingements of the molten particles on the substrate complete the overall character and properties of the sprayed layer [10].

2.3.1 Powder Transport, Flight Path and Velocity of the Sprayed Particles

Transport properties are determined by the shape and size of the sprayed powder particles. A powder suitable for plasma spraying should exhibit acceptable pouring properties, it should soften easily in the plasma beam and the powder particles should be of spherical or similar shape and their size should be as uniform as possible. The spraying of powder with particles of different sizes causes overheating and eventually the evaporation of finer fractions and an insufficient heating of coarse particles may occur. Since the plasma forming gases do not supply the thermal output to the heated powder at the same rate, and since the powder dwells in the plasma a very short time (10^{-4} - 10^{-2}), the point of the powder inlet to the plasma beam is critical [11]. The highest efficiency of powder heating is achieved when the powder is fed to the center of arc burning between the cathode and anode of the torch [12]. However,

such a solution is rather complex from the viewpoint of design, and therefore, in the majority of modern equipment, the powder transported by the carrying gas flow enters the plasma beam radially, from the outside of the nozzle- anode (Fig. 2.5).

A powder particle, thrown perpendicularly into the plasma jet axis, follows a flight path determined by many factors. The beam of particles, moving towards the substrate, has a conical shape with γ angle and it is inclined to plasma axis by angle 'h'. This angle depends on the inlet velocity of particles into plasma beam, their size, the plasma beam velocity (which directly affects the velocity of the particles) and the distribution of velocity in the plasma beam cross section at the point of entry of the particles. Minimum value of h angle ensures favorable spraying conditions since under these circumstances the number of grains moving on the external, colder paths of the plasma beam decrease. The shape of the particle path is thus decisive for the spraying efficiency. The path of the particle flight depends on a great number of factors. The geometry of the plasma torch and powder injector, type and flow rates of the plasma carrying gases, arc output, plasma beam stability are the most important ones [6].

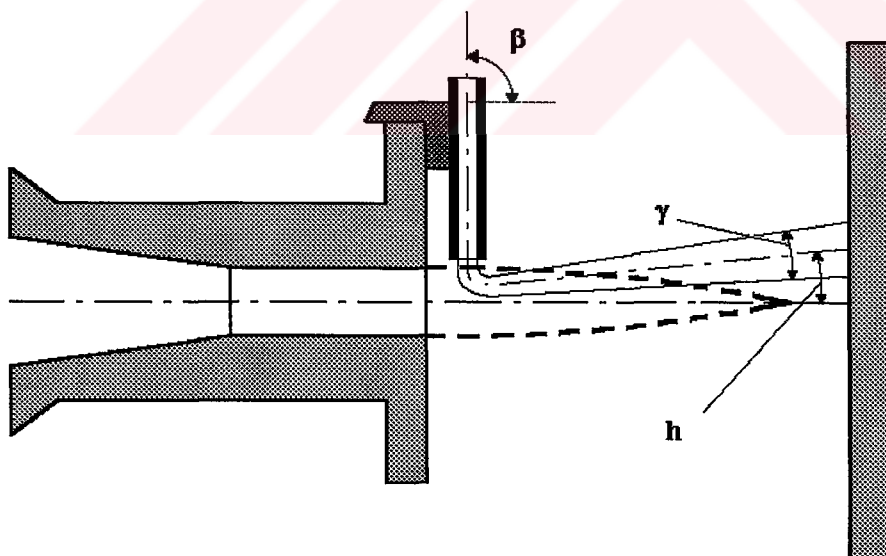


Figure 2.5 Inclination of beam of molten particles

2.3.2 Interactions of Molten Material with the Plasma Beam and the Surrounding Atmosphere

Due to the thermal and kinetic effects of the plasma beam, the supplied powder is melted and accelerated. In the mechanism of heat transfer from plasma beam to powder it is supposed that the energy q supplied to the powder is proportional to temperature, length of the thermally active zone of plasma beam and heat transfer coefficient; and it is indirectly proportional to the plasma beam velocity according to relationship

$$q = \frac{T \cdot \alpha \cdot l}{v} \quad (6)$$

where, q - effective thermal output,

α - heat transfer coefficient,

l - length of thermally active zone of plasma beam,

T - plasma beam temperature,

v -plasma beam velocity.

According to this relationship the cause of insufficient heating can be either not enough time of powder dwell in the plasma ($\tau=1/v=10^{-2} \pm 10^{-14}$ s), insufficient intensity of heat exchange between the plasma and powder, or the problems connected with powder supply to the high-temperature zone of the beam [13].

During the particle flight in plasma, interactions of particles with the gases of surrounding atmosphere and the plasma take place, since all materials at or close to melting temperature exhibit high chemical activity. Of the several mechanisms of interactions of the sprayed particles with the gases, it can be mention the gas adsorption, the chemical interaction and formation of oxide layers and other bonds on the particle surface, the gas dissolution in the molten metal of particle, and the diffusion processes and the mechanical mixing of the interaction products in the particle volume [12].

2.3.3 Impingement of Flying Particles on the Substrate

At the point of impingement of the flying molten particles on the substrate, their kinetic energy transforms into thermal and deformation energy. When particles contact the substrate, they supply their heat to the local part of the surface; cool fast and then solidify. Their behavior in that instant depends on their temperature, velocity and cooling rate. It is known that the kinetic energy at the particle impingement causes their deformation (Fig. 2.6). When spraying parameters are correctly selected the layer of molten particles is formed, depending on the method of spraying, the equipment design and the properties of the filler material [1]. The particles, assuming spherical shapes during their flight due to surface tension, are considerably deformed at impingement, losing their kinetic and thermal energy and then solidify as lamels or nuggets.

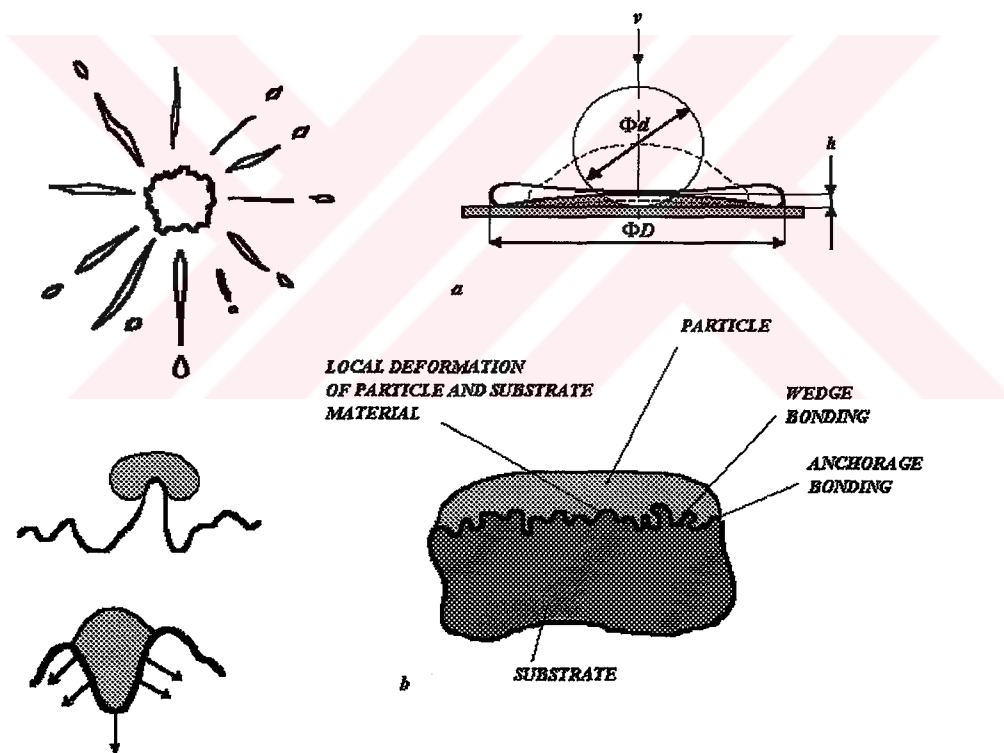


Figure 2.6 Particle deformation on the substrate
a- on a smooth substrate, b- on a rough substrate

As the lamels are deposited on one another, a characteristic lamellar structure formed. The degree of deformation and thus the shapes of lamels depend upon several factors, such as the viscosity and wettability of the molten particles, conditions of their

cooling, powder granularity, character of substrate surface etc., [10]. The molten droplets impinging on a smooth glass surface for example burst rapidly and spread over the substrate surface (Fig 2.6a). On the other hand, a rapid spreading of droplets on a surface roughened by blasting is inhibited by fast cooling and surface roughness, and the solidifying droplets are captured in the surface unevenness (Fig 2.6b). The cooling and solidifying particles individually forms a heterogeneous structure. Other boundaries between the deformed particles and between the individual layers (Fig 2.8) are added to the boundaries typical for the compact materials. The conditions for boundary formation between the layers differ from the conditions for boundary formation between the particles, mainly as concerns the time of duration of contact with the atmosphere. As individual layers are sprayed on the preceding layer, gas is absorbed and the finest fraction of the sprayed material evaporates. At the particle impingement not all particles meet the conditions of deformation and bonding with the substrate or the preceding layer. Some may rebound from its surface or be deposited on it as a non- molten powder, causing thus the defects and pores as well as the material losses and increased portion of non- deformed particles. All these phenomena and the peculiarities of layer formation during the spraying result in the fact that the strength of metal coatings, for example, attains only 10-20 % of that of the similar compact material [14].

2.3.4 Thermal Effects of the Substrate and the Sprayed Layer

The heat transferred to the substrate during spraying consists of the heat transferred by the plasma beam, Q_p and that transferred by the particle, Q_m . The total volume of heat transferred to the substrate in time unit - Q - increases linearly with the input to the torch, and it decreases rapidly at greater torch- work distance [5].

2.3.5 Physical and Chemical Transformation of Material in Spraying

In plasma spraying, the sprayed particles react with the gases of the surrounding environment and the plasma gases. This may cause transformations of the sprayed materials as a result of a number of physical and chemical processes. The contents of O_2 and N_2 in the layers of these materials are given as percentages in

Tab. 2.1 [6].

As seen in the table, the content of dissolved gases approaches the content of gases in the initial material only in case of spraying in an inert chamber or after the heat treatment of layers.

Table 2.1 The contents of O₂ and N₂ in the layers of the sprayed materials

Material spraying conditions	Gas content (%)	
	O ₂	N ₂
TUNGSTEN		
Initial condition	0.113	0.0017
In a layer	0.814	0.024
After heat treatment at 2200 °C in vacuum during 2 hours	0.011	0.0005
Initial condition	0.019	-
In a layer sprayed in Ar chamber	0.044	-
In a layer sprayed in chamber with Ar + 5% H ₂	0.0078	-
MOLYBDENUM		
Initial condition	0.052	0.0033
In a layer	1.02	0.103
In a layer after heat treatment at 2200 °C in vacuum during 2 hours	0.071	0.0001

2.4 Basic Properties of Plasma Sprayed Coatings

The plasma spraying coatings acquire properties differing from those of the initial compact materials: oxygen and nitrogen contents are increased, and the density and plasticity are lowered. These properties are affected by many technological parameters.

2.4.1 Structure

Molten particles in a plasma beam acquire a spherical shape as the result of surface tension. After impingement on the surface, the molten particles of the sprayed material are deposited on one another, similar to pancakes or as lamels until the coating is formed. The kinetic energy of flying particles is transferred into heat.

The plasma sprayed layers have a structure totally different from that of the similar compact materials. Thus the sprayed layers also exhibit different mechanical and physical properties. The chemical composition changes, the burning out of some elements occurs, and oxygen and nitrogen or argon contents increase. The properties of the deposited coating are affected also by many other factors such as the equipment used and the kind of gases used.

The internal structure of the coating is not homogeneous and usually consists of grains of different sizes, adhering to each other. The coatings of molten particles formed are characterized by a layered structure. The structures of layers of molten and solid phases differ a little from the structure of compact materials. The structure of a plasma coating obtained from molten particles is metastable, when heated tries to convert into an equilibrium state [13].

Due to annealing at the metal recrystallization temperature, the lamellar structure changes into a globular one. Unlike coatings sprayed in the atmosphere, it is free from inclusions and oxides [15].

2.4.2 Density and Porosity

Porosity is one characteristic feature and structural guide of sprayed coatings. The more viscous and the faster the velocities, at which the particles are sprayed, the denser is the coating structure and lower the porosity. The pores occur on the grain boundaries.

The microporosity of the coatings is connected with releasing of oxygen, nitrogen and hydrogen, due to their reduced solubility during temperature decrease. The dissolved gases can either escape into free atmosphere (open porosity) or into the microvoids (enclosed porosity). The formation of microvoids results in total porosity of the coating, that is distributed along the particle boundaries or even in the particle themselves. With all probabilities, this porosity determines the maximum coating density and in most cases it can not be removed even if the sprayed part is heated sufficiently. Only the open porosity can be substantially affected by changing the energy conditions of spraying. The enclosed porosity is caused by the gases dissolved in the particles [16].

2.4.3 Bonding, Internal Stresses

The sprayed layer adheres to the substrate surface mainly because of the combined actions of mechanical bonding, valency forces and Van der Waals forces. In metallic coatings sprayed on metals, and ceramic coatings sprayed on ceramic surfaces, diffusion processes take place.

In the process of forming a sprayed coating, compressive and tensile internal stresses meet. These may result in the coating's cracking or peeling off the substrate or, in the case of a thin substrate, the coating may become distorted [17, 18].

The formation of these internal stresses is the result of a non- uniform distribution of the deposited material and a non- uniform heating of the part due to local variations in the action of the plasma torch. The characteristics of the shape and size of the sprayed part also contribute to this field of stresses. The internal stresses on the coating surface formed when the part cools to ambient temperature. When the coefficient of thermal expansion of the sprayed material is equal to, or greater than that of the substrate material, as a result of this, compressive internal stresses are formed in the sprayed material [19].

During spraying, the substrate can be either preheated or cooled in order to reduce the internal stresses. The internal stresses formed can be compensated by use of interlayers [17].

2.4.4 Strength, Hardness

The strength of the coating depends on many factors. The thickness of the coating itself is one of the most important factors. Stress analysis has shown that with the increasing coating thickness and the resulting piling of stresses, the strength decreases [17].

Hardness is often an important characteristic of sprayed coatings. It is directly affected by coating density, and it increases with increasing coating density [6].

2.5 Bonding and Adherence of Plasma Coatings to the Substrate

2.5.1 Kinds of Bonding Forces

The term, 'adherence' denotes the sum of surface forces by which particles of different mass attract each other. From the viewpoint of plasma spray technology, this term is used also to designate the force necessary to tear off a unit area of coating from the substrate. The effects of following factors acting to create adherence are:

- a) mechanical bonding of molten particles into the substrate;
- b) contribution of physical interaction forces of the Van der Waals type;
- c) chemical interaction leading to microwelding of particles, i.e. formation of strong chemical bonds of a covalent or metallic type;
- d) metallurgical processes, taking place in close vicinity to form microwelds.

The formation of a chemical bond is probably caused by the interaction of the electron envelopes of atoms. When metal is deposited on metal, the quantum

processes of electron interaction lead to agglomeration of valence electrons, and then the creation of a common lattice. When non-metallic coatings are deposited on metal, covalent or coordination-covalent bonds can occur if both materials are bonded with each other.

There are also contradictory opinions on the principles of bond formation between the coating and substrate. In some works, the scientists state that the time of interaction at high temperature is too short, and therefore they suppose that the principal role in the process of bond formation is played by mechanical catching of the coating mass, on the microunevenness of the substrate. Two variants of this type of bonding are distinguished (Fig. 2.7):

- a) wedge catching, when the size of microunevenness of the substrate is smaller than that at the elevation peak and the bond is formed by friction forces only;
- b) anchor catching, when the microunevenness differentiates at its base. The anchor type of catching, providing the strongest bond of coating and substrate, requires maximum viscosity and velocity of the sprayed particles.

Many scientists believe that the bond of substrate and coating is conditioned by mechanical catching, as well as by the formation of chemical bonds between the coating and substrate and the formation of forces of physical interaction. The importance of individual bond types may thus change, depending on the selection of materials of coating and substrate, their properties and the technological parameters of spraying. Mechanical bonds prevail when ceramic coatings are sprayed on metal, but metallic bonds predominate between metal coatings and metal bases [6].

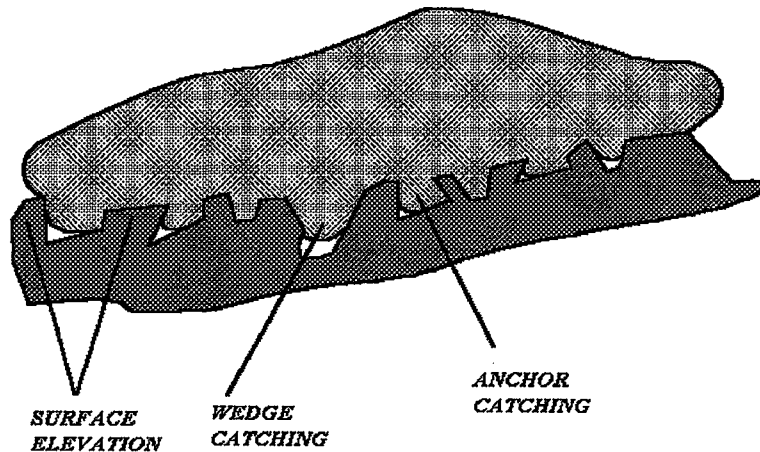


Figure 2.7 Types of coating bonds with substrate

2.5.2 Metallographic Analysis of the Bond

The quality of the bond between a sprayed coating and a substrate is studied by light and electron microscopy of the structure of a metallographic sample. The structure of a plasma sprayed coating consists of the deformed particles of deposited powder, composed of thin plates- lamels bonded together by the welded sections, and bonding by F_x areas, (Fig 2.8) formed during the solidification of particles on the contact surface. The welded sections do not cover the whole contact area between the particles; therefore the strength and density of the coatings are lower than those of the compact material.

The processes of impingement, deformation, solidification and cooling, as well as the physico- chemical interactions of the plasma beam and its surrounding environment during transport to the substrate, determine the structure and properties of the coating. A number of structural components (Fig 2.8) observed in the individual zones of interface can be separated. The interface between the coating and the substrate (1) determines the strength of their bond (coating adherence). The

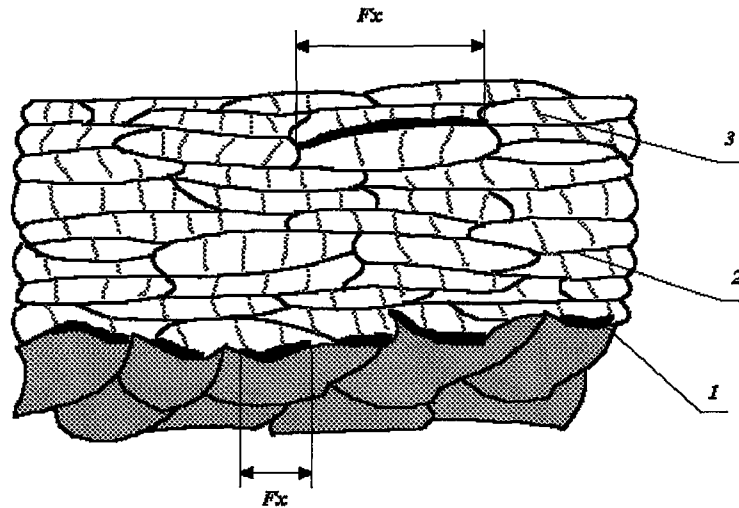


Figure 2.8 Coating structure

1- boundary between the coating and the substrate, 2- boundary between the individual layers, 3- boundary between the particles. F_x - diameter of surface area where welding of particles occurred.

interface between the individual layers formed by one pass of the spraying torch (2) is formed at different times.

During the deposition of individual layers, the surface is contaminated and the contact processes below the particles deteriorate. Into interface of sections between the particles in the layer (3), the area of contact surface at the points of bonding F_x penetrates and, in those zones, the individual particles are welded on the coating (Fig 2.8). The zones of welding determine mechanical properties of the coating.

The interface between the layers of the coating can be evaluated by light and scanning microscopy. If this interface is not definite, or if it contains agglomerated pores or a continuous thick interlayer, then its poor quality is caused either by improper preparation, surface contamination, oxidation or delamination of the coating by unsuitable spraying procedure. The distinct and thin interface between

the deposit and substrate shows the perfect adherence of every particle to the substrate unevenness [5].



CHAPTER 3

EXPERIMENTAL SETUP AND PROCEDURE

3.1 Plasma Spraying Equipment

In making the experiments, the basic equipments of Metco Perkin Elmer were used.

3.1.1 Metco 9M Plasma Spray System

A complete METCO 9M plasma spray system requires the use of a type 9MC plasma control unit, type 9MCD distribution unit, and the following equipment [2]:

- Type 9MB Plasma Spray Gun
- Type 9MR Power Supply Unit
- Type 9MP Powder Feed Unit
- Cooling Equipment
 - Water Booster Pump
 - Heat Exchanger
- Hose and Cable Unit
- Nitrogen/Argon/Helium Gas Regulators
- Hydrogen Gas Regulator
- Type 5A Air Control Unit
- Air Cooling Unit
- Spray Booth
- Industrial Spraying Robot

i) Type 9MC Plasma Control Unit

The METCO type 9MC Plasma Control Unit provides automatic operation, monitoring, and control of the METCO type 9MB Plasma Spray Gun. The control unit along with the distribution unit, controls various functions of the entire 9M Plasma System. The control unit is composed of three distinct cabinets:

- a) System status monitor
- b) Gas flow control
- c) Electrical control

The unit contains all of the controls necessary to automatically start and stop the operation of plasma system. It continually meters and maintains preset gas flows to the gun and automatically starts material feed. The control unit continuously monitors the supply pressures of the primary gas, secondary gas, carrier gas and air. The unit will shut the system down automatically in the event that any pressures go beyond safe operating levels.

ii) Type 9MB Plasma Spray Gun

The gun is made up of a nozzle, a water channeling head, electrode, insulator assembly and a gun mount assembly. It can be set up to use either argon or nitrogen as the primary plasma gas. It is supplied with a standard argon front insulator (two gas holes) installed. A nitrogen front insulator is also furnished. Both insulators can be used for power levels up to 80 kW.

iii) Type 9MR Power Supply Unit

The type 9MR power supply unit is a high power rectifier developed specifically for the automatic system. It is fully SCR controlled and delivers a constant current, even with the power line fluctuations and different cable lengths. The unit is equipped with 3 phase line and thermal overload protection. All the operating functions are constantly monitored by the control unit during operation. A main

control unit breaker prevents internal damage in case of a 3 phase line imbalance. Fuses are provided for the fan motor control circuits. The oversize fan forces air circulation through the system components to allow operation up to 88kW.

iv) Type 9MP Powder Feed Unit

The type 9MP powder feed unit is a self contained device providing complete metering, monitoring, and closed loop control of powder feed rate. It incorporates a fluid bed powder regulating system for consistent feed control of a wide range of coating materials.

v) Type 5A Air Control Unit

It controls pressure flows, and filters the compressed air to the control unit that will be used later for cooling the part during spraying.

vi) Spray Booth

To protect personnel in the vicinity of the spray operation against excessive noise, and to dispose of gas and fumes we have a suitable spray booth with an adequate exhaust system.

vii) Industrial Spraying Robot

In this study, for spraying operations, a special robot for plasma torch guidance, named Metco Standart Robot, was used. It is a robot of articulated design with six axes of freedom, whose movements can be transformed onto rectangular coordinates. The motion system of the manipulator consists of a base stand rotating around axis (1), a lower arm 630 mm long rotating around axis (2) an upper arm 800 mm long rotating around axis (3), and a joint wrist rotating or tilting along axes (4), (5) and (6). Motion of all axes can be controlled simultaneously and all joints can be interposed and started or stopped instantaneously. An electric servo system employing a DC motor, replacing the conventional hydraulic drive, drives the machine. The

plasma torch with a maximum weight, fixed in the joint arm, can move along the programmed path at 1500 mm/sec speed and reproduces the given position with 0.5 mm accuracy. A complex robot system consists of the manipulator proper, control box, control unit, portable control unit, and programming module with the keyboard and display. The robot is controlled by a unit operated according to cartridges, or are provided by the printer. The program memory has a standard capacity of 1000 positions, but can contain up to 6000 positions. The microprocessor-controlled box of the plasma spraying equipment can be functionally linked with the robot control, or with the control of clamping mechanism for the sprayed parts, and in this way, the programmed process of plasma spraying of parts with intricate surface geometry is ensured [2].

3.1.2 Abrasive Cleaning Equipment

In this equipment, the manually adjustable throwing head throws the abrasives on the treated part fixed on a rotary table in a cabin. The machine is connected with an industrial exhaust cleaner that removes the dust inside the cabin. The abrasive material is drawn out of a supply container by the ejection effect of pressurized air into a Venturi chamber. The abrasive material is then supplied to a nozzle by pressurized air and thrown on the treated surface at high velocity. The abrasive material recirculates in a closed circuit [4].

3.2 Procedure of Plasma Spraying

3.2.1 Preliminary Preparation of Surfaces Prior to Spraying

Preparation prior to spraying is important for ensuring a strong bonding of the sprayed coating with the substrate material, since the bond is mostly of mechanical character. The surface must be sufficiently rough in order to catch the sprayed particles in its unevenness. Also other types of bonding such as microwelding of particles with substrate, formation of chemical bonds, etc., exist. These types of bondings require enlargement of the contact area and activation of the surface. Optimum conditions for forming a strong bond can be guaranteed by removing

moisture, grease and oxide films and by providing a suitable roughness. According to actual exploitation of the plasma sprayed coating also mechanical machining of surface by turning, machining, chemical degreasing and cleaning as well as roughening of the surface by abrasives [3].

3.2.2 Chemical Degreasing

Adherence of sprayed coatings is impaired by any grease on the surface of the material. The most common way to remove grease is to use chemical solvents. Mineral oils can be removed by washing the parts or by using the vapors of chemical solvents like trichlorethylene, acetone, etc. [5].

3.2.3 Abrasive Cleaning

This method uses the kinetic energy of high-speed abrasive particles to remove impurities, paint residues, scales, rust and oxide film from the surface and assures the surface roughness and surface activation that increases the gravitational forces between the atoms of the surface and the sprayed layer. These are the conditions necessary for the optimum adherence of sprayed coatings to the substrate [5].

3.2.4 Application of Interlayers Improving Adherence

By spraying special materials on clean and pretreated metallic substrates, a suitable underlayer for the next plasma sprayed coating can be obtained. Such interlayers are characterized by good adherence of the next plasma sprayed coating. Moreover, interlayers compensate for the very different thermal expansion coefficients of the substrate and the material of the working layer by lowering the shear stresses formed on the boundary of substrate and layer. Great differences in thermal expansion coefficients occur between ceramic layers and metallic substrates. The interlayers may also serve other specific purposes, for example, protecting the substrate from corrosion, gas formation, the effects of high temperature, etc. In this study Ni-Al coat was used as an interlayer [20].

3.2.5 Working Parameters of the Spraying Process

Electric input of the plasma torch, torch- substrate distance, plasma gas volume, amount and granularity of the sprayed powder are accepted as the basic parameters of the plasma spraying process after a lot of works done in this branch [1, 2, 3, 5, 6].

i) Abrasive Cleaning

On all the test coupons and buttons, surface roughness was measured between 80-150 RA after the application of Abrasive Cleaning Operation [21].

ii) Masking

Non- functional surfaces were masked during the tests. For example, in case of test buttons for tensile testing, edges of those to prevent extra cleaning were masked with heat resistant masks during the spraying.

iii) Preheat and Cooling

In principle, there are three reasons to preheat the work: to remove moisture or condensation from the substrate, to improve the adherence conditions and to balance the different thermal expansions of dissimilar materials, moderate preheat was applied on coupons to 80-100⁰C. Also air cooling was used to prevent the overheating of the coupons because of the high thermal output of the plasma beam and heat transfer from the impinging molten particles (Except last three tests of the study to see the effects of preheating, time of exposure of preheating was changed) [7].

iv) Spraying of Parts

Plasma spraying were started after the following operations were completed in the given sequence: pretreating surface, cleaning abrasive grains from

the surface, masking of non-functional areas, clamping of test coupons on rotary table, setting of torch travel speed (torch travel speed is controlled by robot) on the coupons, setting of working parameters of plasma equipment, preparation of measuring instruments, measurement of initial size of the part to be sprayed and preparation of cooling of the part. After through surface pretreatment, the surfaces were cleaned, by a jet of compressed air that removes all dust and abrasive grain residues. During the tests, optimum spraying angle of 90° that provides dense and good quality coating was used.

Plasma equipment was prepared by setting the output gas pressure on the pressure cylinder valves and setting the gas feeder and the working parameters of spraying. The output pressures of primary (argon), secondary (hydrogen) and carrier (argon) gases were set to 75, 50 and 60 psi values. After that, the desired powder supply in the tests was set by the volume of powder carrying gas and vibration of the hopper that contains powder. After the plasma arc and the powder feeder start, the preselected parameters (flow rates of plasma gases, current and voltage, etc.) were set. At the end the robot arm was operated to make spraying in a desired path, distance and number of passes (one pass is the one forward and backward travel of the plasma torch on the part while rotary table is rotating at the specified speed).

At last, after coupons reached the coating thickness of the desired level, (it is determined by measuring instruments after some number of passes) the operation was stopped and they were carefully taken for inspection.

3.3 Materials

Powder used in this study was Triballoy 400 (GE specification B50TF155, Cl A). It contains Cobalt- Molybdenum- Chromium- Silicon Powder, and is called Low Temperature Hardcoat. Its composition is as follows: Molybdenum (27.00-30.00%), Chromium (7.50-9.50%), Silicon (2.20-3.00%), Iron Nickel (3.00% max), Carbon (0.08% max), Phosphorus (0.03% max), Sulfur (0.03% max), Oxygen (0.15% max) and Cobalt remainder.

Powder, that was used as an interlayer (bond coat) in some of the experiments, was Nickel Aluminium Thermal Spray Powder (GE Specification B50TF56 C1A). It contains Aluminum (4.00- 5.00%), Nickel (93.00% min), Organic Solids (2.5% Max) and total other elements (1.00% max).

In this study, the substrate material was the Nickel base alloy (Inconel 718), and a synthetic corundum (Al_2O_3) was used as an abrasive cleaning material.

3.4 Test Specimens

In each experiment, 5 test specimens were used: one for microstructural examination, one for hardness and three for tensile strength measurements of the coatings. Test specimens, also called 'test coupons', that were used for the microstructure and hardness evaluations, were 1.50 inches in length, 0.75 inches in width and 0.060 inches in thickness. The tensile specimens, also called 'test buttons' had dimensions of 1.00 inch diameter and 0.25 inches of thickness.

The thickness of the coatings was measured by flat anvil micrometer. It was determined as an average of three measurements made at three different locations on the test coupons and all measurements were made to the nearest 0.001 inches [21].

3.5 Tensile Bond Strength Test

Tensile strength is defined as the stress necessary to tear off the coating. For each test, the tensile bond strength value was determined from the average of three coated specimens that have 0.09 inches minimum thickness. All test specimens were processed through the same coating surface preparation and coating application procedures. The surfaces of the test specimens that are not coated were masked, and all overspray was removed after coating.

Test specimens were assembled using an adhesive bonding agent that has a tensile bond strength over 2500 psi. After curing, any residual adhesive on the surfaces adjacent to the bond area were removed [21].

The tensile bond strength tests were carried out by applying a tensile load to each test specimen at a constant rate between 1200 to 1400 psi per minute until rupture occurs. In case of complete penetration of the adhesive through the coating occurred in any area, the test was considered invalid. All the tests were performed at room temperature.

3.6 Hardness Measurements

In this study, Rockwell equipment (in 15N scale) was used, in the evaluation of the surface hardness of the test coupons that had a minimum coating thickness of 0.018 inches after spraying.

One of the difficulties associated with sprayed coatings was that their hardness was highly variable. This may be the result of the peculiar laminar structure of the coating. Thus, the arithmetic average, rounded off to the nearest 0.1, was determined from the results of ten sequential readings on the prepared coating surface [22].

Before surface hardness testing, the as-coated surface was abraded to take uniform hardness values throughout the coat. Attention was given to have at least 0.015 inches of coating thickness after grinding.

3.7 Evaluation of the Microstructure of the Coatings

The evaluation of the coating microstructure was performed in the as-polished and unetched condition at the magnifications according to General Electric photo standards. It was accomplished by scanning the specimen under the microscope at the appropriate magnification and determining which of the photo standards most nearly fits the views observed. The characteristic letters used to designate the quality of microstructure of coating were as follows [21]:

i) Voids and Porosity:

V1: Good, V2: Fair, V3: Bad, V4: Worst.

ii) Oxide Level:

X0: Good, X1: Fair, X2: Bad, X3: Worst.

iii) Interface Between the Coating and the Substrate:

I0: Good, I1: Fair, I2: Bad, I3: Worst.

iv) Unmelted Powder:

U0: Good, U1: Fair, U2: Bad, U3: Worst.

The samples for microstructural evaluation were prepared by standard metallographic techniques. The structure was studied in cross sections vertical and oblique to the coating surface. The surfaces of specimens were wet ground on emery papers with 150 to 600 μm , and polished with diamond pastes with 5 to 1 μm granularity whereby special attention was developed not to peel off the coating.

3.8 Experimental Program

As mentioned before, recommended parameters of plasma spraying process on the mechanical properties of the coating can be stated as: electric input to the plasma torch (nozzle), amount of plasma gases, amount of powder and torch-substrate distance.

Furthermore, the effect of substrate temperature should be considered which is also affected by preheating, gun to substrate distance, plasma gas composition, plasma energy and substrate characteristics [15].

In this study, six basic plasma spray parameters were chosen to see the outcome of all these effects (Table 3.1):

1) primary and secondary gas flows are the constituents of the total plasma gas.

Generally, they affect the voltage, and the electric input (voltage.ampere) used in the process,

2) carrier gas flow of powders: The carrier gas transports powders from hoppers to the torch tip. And its spray rate would determine directly the amount of powder supplied.

- 3) torch tip- test specimen distance, and
- 4) preheating of the test specimens, which is the primary effective parameter on the substrate temperature.

To determine the effects of all these parameters on the microstructure, tensile strength and hardness of the coatings, 14 tests were conducted. The first test was done by using optimum parameters established by several tests. To evaluate the effect of each parameter, at least two tests were done, one is about 20% more, another is 20% less than the optimum parameter. For example, in the case of distance, optimum value was 4 inches; and accordingly the other two were selected as 3 and 5 inches. Other parameters were also chosen by using the same logic.

Some parameters were kept constant throughout the whole experimental program. These were; turntable speed (85 RPM), air cooling pressure (80 psi), traverse speed of torch during spraying (3.4 mm/sec), spraying angle (90°), nozzle type (732).

Some additional tests were conducted to see the effect of electric input, spray rate and spray distance on the hardness behavior of the Co-Mo-Cr-Si coat that contains an interlayer. The test values were given in Tables 3.2, 3.3 and 3.4.

Plasma spraying parameters of B50TF56 Cl-A type bond coat are given in the Table 3.5:

Table 3.1 Test parameters

Test No	Primary Gas Flow (scfh*)	Secondary Gas Flow (scfh)	Voltage (Volt)	Carrier Flow (scfh)	Spray Rate (gr/min)	Spray Distance (inches)	Number of Preheat Passes
1	140	24	77	11	45	4	1
2	120	24	73	11	45	4	1
3	160	24	80	11	45	4	1
4	140	20	75	11	45	4	1
5	140	30	80	11	45	4	1
6	140	24	77	7	45	4	1
7	140	24	77	15	45	4	1
8	140	24	77	11	30	4	1
9	140	24	77	11	60	4	1
10	140	24	77	11	45	3	1
11	140	24	77	11	45	5	1
12	140	24	77	11	45	4	0
13	140	24	77	11	45	4	2
14	140	24	77	11	45	4	4

* Standard cubic feet per hour.

Table 3.2 Change in Electric Input

Test No	Primary Gas Flow (scfh)	Secondary Gas Flow (scfh)	Voltage (Volt)	Electric Input (kW)	Carrier Flow (scfh)	Spray Rate (gr/min)	Spray Distance (inches)
1	140	5	58	29	9	30	3.7
2	140	8	62	31	9	30	3.7
3	140	12	65	32.5	9	30	3.7
4	140	16	70	35	12	45	3.7
5	140	22	76	38	12	45	3.7
6	140	28	80	40	12	45	3.7

Table 3.3 Effect of Spray Rate

Test No	Primary Gas Flow (scfh)	Secondary Gas Flow (scfh)	Voltage (Volt)	Carrier Flow (scfh)	Spray Rate (gr/min)	Spray Distance (inches)
1	140	8	62	10	40	3.7
2	140	8	62	10	45	3.7
3	140	8	62	10	60	3.7
4	140	8	62	10	80	3.7
5	140	8	62	10	100	3.7

Table 3.4. Effect of Spraying Distance

Test No	Primary Gas Flow (scfh)	Secondary Gas Flow (scfh)	Voltage (Volt)	Carrier Flow (scfh)	Spray Rate (gr/min)	Spray Distance (inches)
1	120	24.5	75	8	30	3
2	120	24.5	75	8	30	3.25
3	120	24.5	75	8	30	3.50
4	120	24.5	75	8	30	3.75
5	120	24.5	75	8	30	4

Table 3.5 Plasma Spraying Parameters of the interlayer type B50TF56 CI- A

Parameters	
Primary Argon (scfh)	95
Secondary Hydrogen (scfh)	18
Amperage	500
Voltage	67
Carrier Flow (scfh)	55
Spray Rate (gr/ min)	50
Distance (inches)	4
No. of preheat passes	1
No. of coat passes	2
Thickness ($\times 0.001$ inches)	4
Nozzle type	732

Another study was done, to see the effects of secondary plasma spraying parameters on the coating quality of an aircraft engine part, whereby their optimum values were established according to microstructural evaluations of the several test coupons. The test procedure applied in this part of investigation is given in the Appendix.

CHAPTER 4

RESULTS AND DISCUSSION

All the results obtained from hardness and tensile tests together with those of microstructural examinations are summarized in Tables 4.1 to 4.6. The effects of various parameters on the quality of coating are discussed as follows.

Table 4.1 Hardness Results (with bond coat)

Electric Input (kW)	Rockwell Hardness (15N)
29	73
31	73
32.5	76
35	76
38	77.5
40	78.5

Table 4.2 Hardness Results (with bond coat)

Spray Rate (gr/min)	Rockwell Hardness (15N)
40	76.5
45	78.5
60	78
80	77
100	75

Table 4.3 Hardness Results (with bond coat)

Spray Distance (inches)	Rockwell Hardness (15N)
3	77.5
3.25	77.8
3.50	78
3.75	79.3
4	79

Table 4.4 Hardness Results

Test No	Rockwell Hardness (15N)
1	80.8
2	79.3
3	79.7
4	79.9
5	80.1
6	78.9
7	80
8	79.8
9	80
10	80.4
11	80.5
12	80.3
13	80.5
14	79.4

Table 4.5 Tensile Test Results

Test No	Tensile Strength (psi)
1	6028
2	5143
3	5423
4	5678
5	4710
6	5124
7	5920.5
8	5379
9	5048
10	5341
11	5334.5
12	4258.5
13	5923
14	4933.5

Table 4.6 Microstructural Test Results (Optical Microscope 200×)

Test No	Void	Interface	Unmelt	Oxides
1	V1	I1	U1	X1
2	V1-V2	I1	U1	X1
3	V1-V2	I1	U1	X1
4	V2	I1	U1-U2	X2
5	V2	I1	U1	X1
6	V3	I1	U2	X1
7	V2	I1	U2	X1
8	V2	I1	U1	X1
9	V1-V2	I1	U2	X1
10	V2	I1	U2	X1
11	V1-V2	I1	U1	X2
12	V2	I1	U1-U2	X2
13	V1	I1	U1	X1
14	V2	I1	U1-U2	X1

4.1 Effect of the Primary Plasma Spraying Parameters on the Properties of the Coating

4.1.1 Effect of Distance

Spraying distance, the distance between torch tip and substrate during plasma spraying, is one of the most important parameter, which directly affects the coating quality. To determine this effect, the properties of the coatings sprayed at 3, 4 and 5 inches were compared (Table 4.4 and 4.5). In a second set of experiments, the hardness of the coatings with an interlayer, were determined (Table 4.3).

As indicated also in Fig 4.1; the highest hardness and tensile strength were obtained at a spraying distance of 4 inches. Same phenomenon can be also seen in Fig 4.2, with similar spraying parameters and the existence of an interlayer; maximum hardness value was reached approximately at the same value.

Below that distance, hardness and tensile strength values drop immediately. The reason is, at shorter distances the plasma beam hits the substrate and overheats it considerably, causing excessively molten particles to splash, creating a less dense, structure which contains excess voids [13].

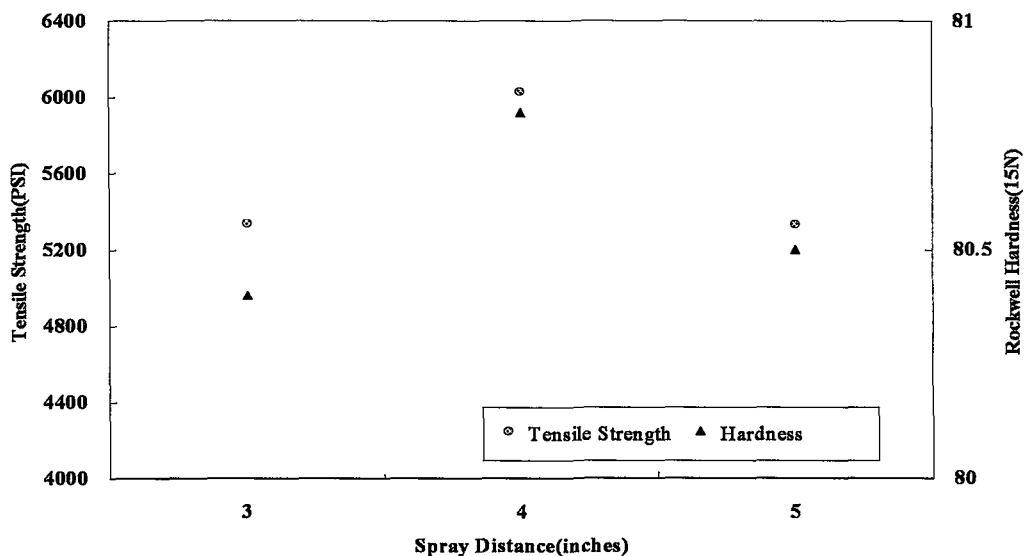


Figure 4.1 Effect of spraying distance on hardness and tensile strength

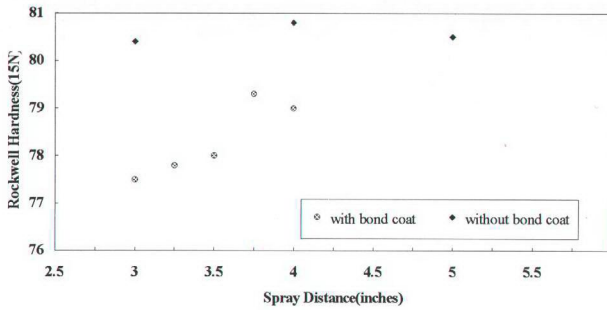


Figure 4.2 Comparing the effects of the spraying distance on hardness of the coatings with and without bondcoat.

A direct proof of this can be created by comparing the microstructure of the coating sprayed at 3 inches (Fig 4.3), to that of the coating produced at 4 inches spraying distance (Fig 4.4).

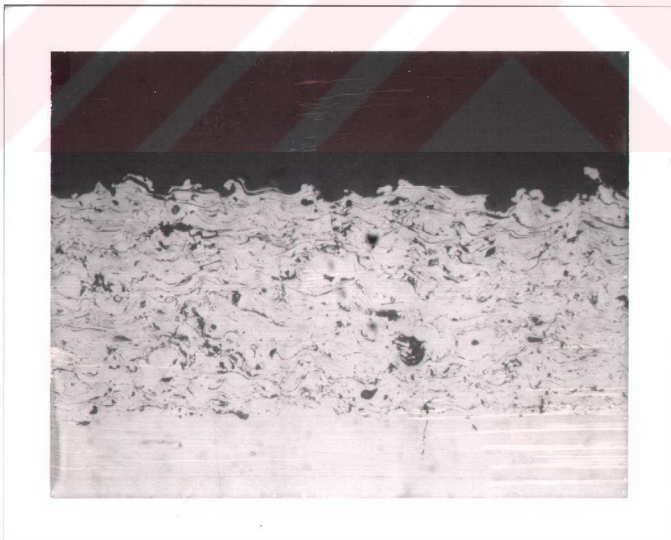


Figure 4.3 Microstructure of the coat, sprayed at 3 inches (200 \times).

As seen from Fig 4.3, the microstructure of the coating sprayed at 3 inches contains more voids and also some unmelted particles. Existence of unmelted particles are due to insufficient dwell time for melting of powders within plasma flame, because of shorter distance [5].

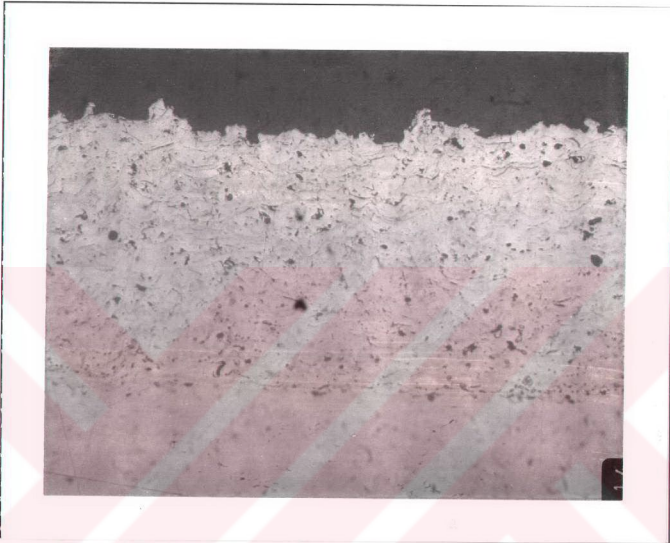


Figure 4.4 Microstructure of the coat, sprayed at 4 inches (200 \times)

At longer spray distances, again lower hardness and tensile strength values are seen. These may be due to the excessive oxide content in the coating microstructure (Fig 4.5). Such an oxide film occurs as a result of the interaction of the powders with surrounding air during spraying. Because, with increasing spraying distance, protective effect of plasma gases (especially argon) on powders during their flight path decreases [13, 23]. Therefore, they can not prevent the occurrence of an oxide skin around the particles during spraying. This oxide skin which forms on each particle is likely to restrict the flowability prior to solidification and thus increases the void content [10]. This means less dense structure of the coating, so lower hardness values [6].



Figure 4.5 Microstructure of the coat, sprayed at 5 inches (200×)

The reasons of lower tensile strengths can be explained as follows:

- 1) The presence of a brittle oxide film at the particle boundaries which impedes particle interaction and can act as a path for crack propagation,
- 2) The existence of large number of interparticle pores which reduce the surface area between the particles, forming 'Bottle-Necks,' and which therefore increase the stress concentration in these regions. Cracks can be nucleated at the pores and can then propagate through the oxide layers, giving rise to failure [10, 18, 19, 24].

4.1.2 Effect of Electric Input and Gas Flow Rate

The electric input supplied to the plasma arc significantly affect the thermal content of plasma gas and thus also the heat transfer to the sprayed powder [2, 5- 7], so the effect of this variable on the microstructure, hardness and tensile strength of the coatings must be considered . There are two ways to change this electric input; one is by adjusting the amperage amount while fixing the voltage level,

and the other is changing the voltage while fixing the amperage. The first one can be done by using a switch in the control unit of the plasma machine. The latter can be adjusted by changing the plasma gas volumes [2], because, there is a direct relationship with plasma gas content and voltage level of this process [2, 5, 8]. With increasing gas content, voltage increases. In this study, electric input was adjusted by using voltage with the help of plasma gas content. The diagram in Fig.4.6 shows the dependence of the given electric input to the arc with tensile strength and hardness of the coating.

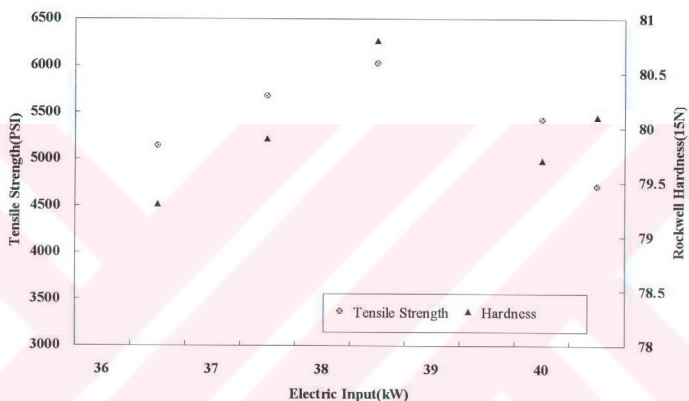


Figure 4.6 Effect of electric input on tensile strength and hardness of the coating.

It can be clearly seen from this figure that the maximum hardness and tensile strength value was attained at about 38.5 kW input.

Fig.4.7, shows the effect of increasing gas flow rate, on hardness and tensile strength of the coating. These results prove the existence of a relationship between plasma gas content and electric input. As seen from Figures 4.6 and 4.7, the highest hardness and tensile strength are obtained at a critical combination of gas flow rate and electric input.

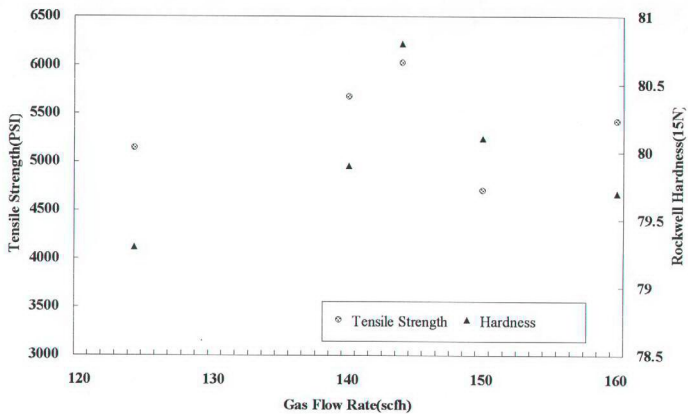


Figure 4.7 Total effect of primary and secondary gas flow rates on tensile strength and hardness of the coating.

The explanation to these variations in both diagrams can be as follows: At lower electric input levels, which was reached at lower gas flow rates, the plasma beam velocity, as well as the velocity of the particles flying in it, decrease. This leads to coatings with excess amount of voids and unmelted particles, because of insufficient heat content, and oxides, due to decreasing protective effect of the gases [2, 13, 16, 23]. This makes low hardness and tensile strength values, as it was described. With increasing gas flow content up to a certain level (144 scfh), electric input increases (up to 38.5 kW) in the same rate and as a result, increasing the velocity of the particles make the structure of the coating more dense and contains less amount of voids. Therefore, the optimum microstructure was reached at 38.5 kW and 144 scfh (Fig 4.4). After those values, deteriorating the microstructure, hardness and tensile strength due to the cooling effect of the gases at high plasma gas volumes [25]. Because, the increasing velocity can not be combined with increasing heat content to melt powders completely while they are being sprayed [6]. As a result, excess amount of void content may occur in the microstructure of the coatings.

These theories can be proven by examination of microstructures of the coatings under an optical microscope (Figs 4.8, 4.9, 4.4, 4.10, 4.11). Excess void contents can be seen at higher and lower gas flow rates (or electrical inputs). In addition, at lower gas flow rates, some unmelted particles and oxides, are observed.

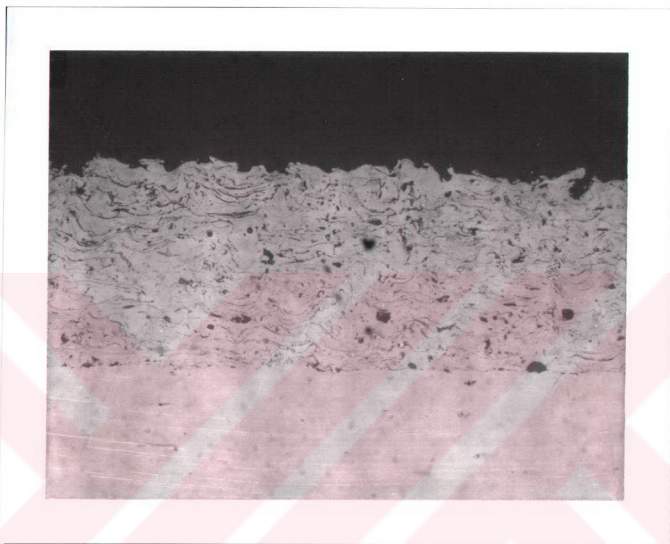


Figure 4.8 Microstructure of the coat, sprayed at 124 scfh gas flow rate (200 \times).

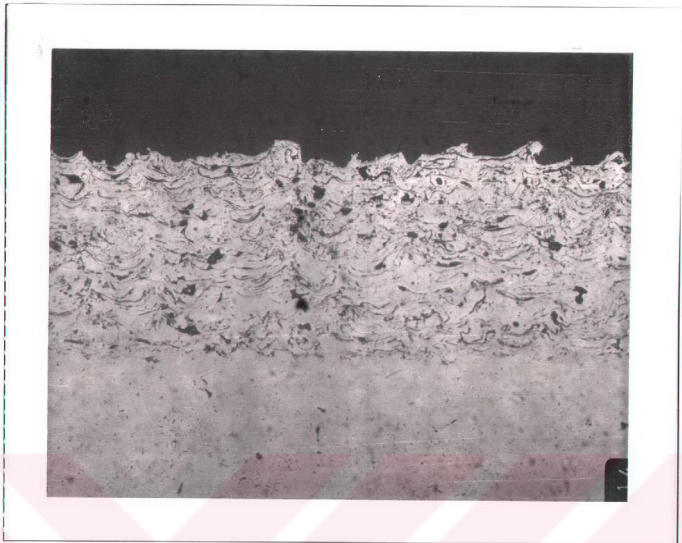


Figure 4.9 Microstructure of the coat, sprayed at 140 scfh gas flow rate (200 \times).

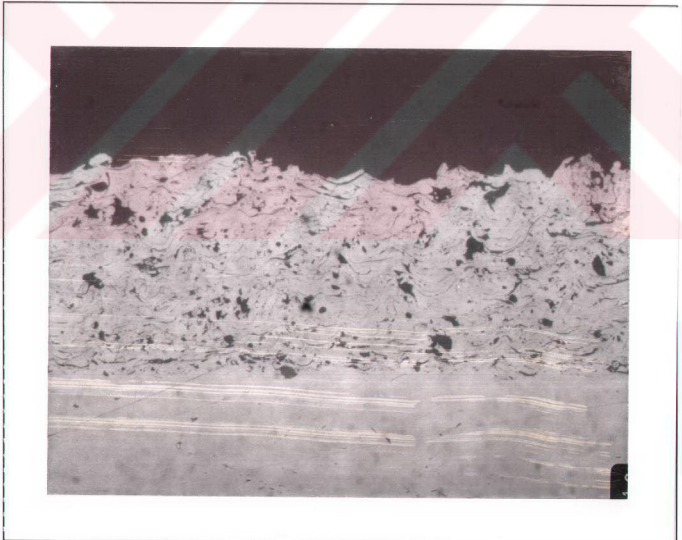


Figure 4.10 Microstructure of the coat, sprayed at 150 scfh gas flow rate (200 \times).

factors that affect directly the inlet velocity of powders into plasma beam. As mentioned before, this inlet velocity influences the angle of the particle beam with respect to plasma beam, h , as can be shown in Fig 2.5 [6]. If this velocity decreases, h will increase, and as a result of this, increasing number of powders moving on the colder paths of the plasma beam may be possible. As can be differed from the results of Tests 6 and 9, the ratio of unmelted powders is the highest, being consistent with the observation that the angle, h , was at its highest value in these experiments (see also Fig 4.12). Therefore, the lowest magnitude of inlet velocity was reached in those cases. The metallographic evaluation under an optical microscope of the coatings, created additional evidence that an excess amount of voids and unmelted particles were included in both coatings, as natural consequences of the low inlet velocity (Figs 4.13, 4.14).

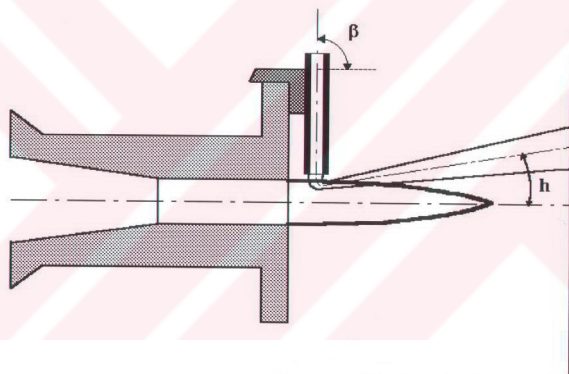


Figure 4.12 With lowering the inlet velocity of the powders, h angle increases.

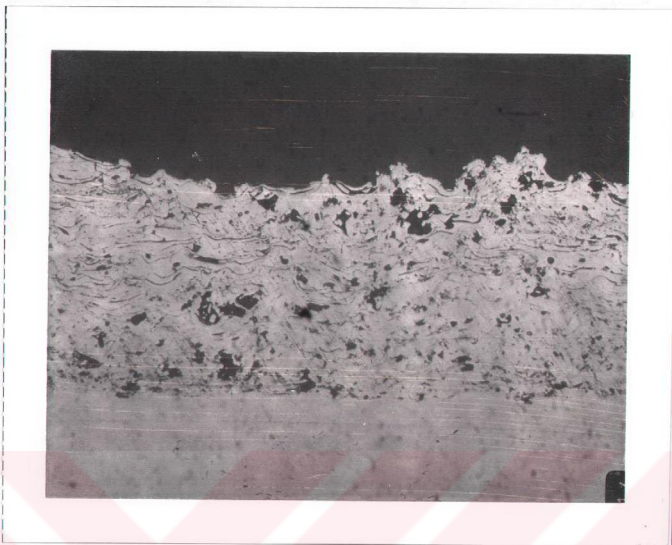


Figure 4.13 Microstructure of the coat, sprayed at 7 scfh and 45 gr/min (200 \times).

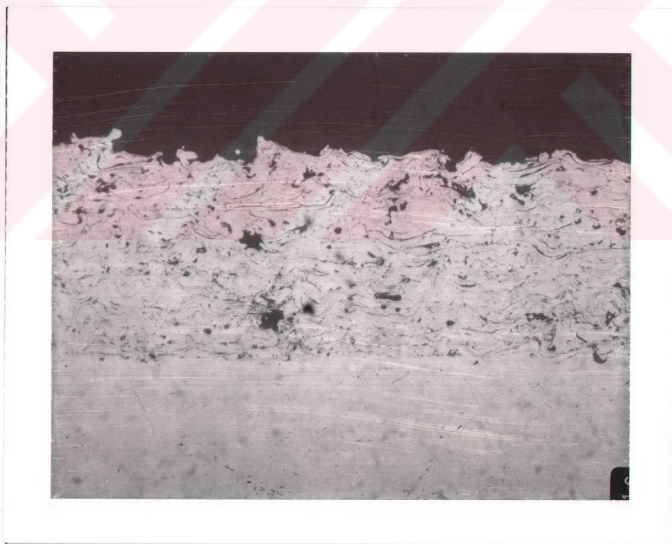


Figure 4.14 Microstructure of the coat, sprayed at 11 scfh and 60 gr/min (200 \times).

Coating procedure carried out under conditions of higher carrier gas flow rates resulted in higher inlet velocities of powder, which is consistent with a smaller value of angle, h . This facts were demonstrated by the tests numbered 7 and 8. Here, due to increasing the carrier gas flow rate, cooling effect of gas (argon) during the trajectory of the particles create an increasing number of unmelted particles and excess amount of voids in the microstructure of these two coatings (Figs 4.15, 4.16) [25].

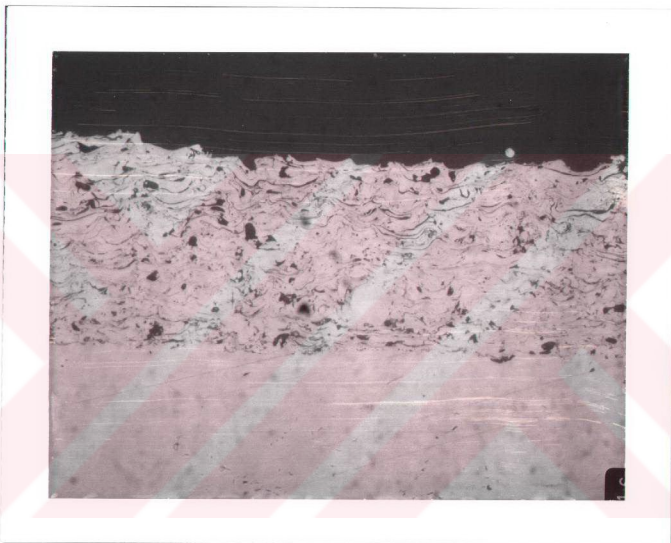


Figure 4.15 Microstructure of the coat, sprayed at 15 scfh and 45 gr/min (200 \times).

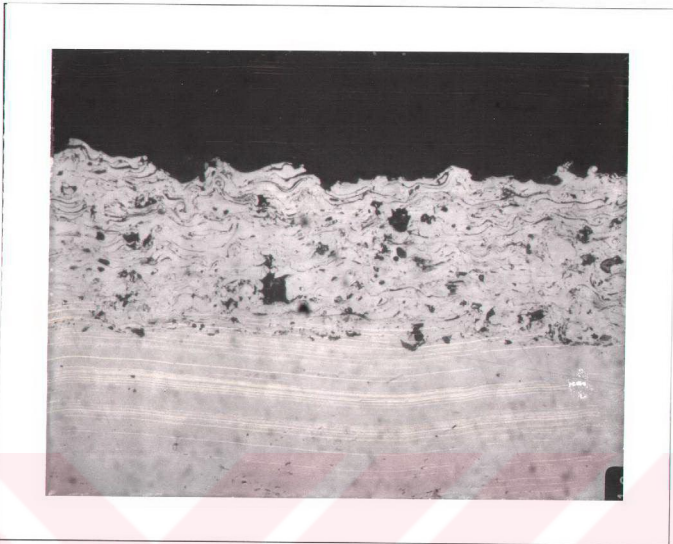


Figure 4.16 Microstructure of the coat, sprayed at 11 scfh and 30 gr/min (200 \times).

The comparison of the tensile strength and hardness values in the diagrams (Fig 4.17, 4.18), reveals that the peak value of both properties were reached at a spray rate of 45 gr/min and carrier flow rate of 11 scfh.

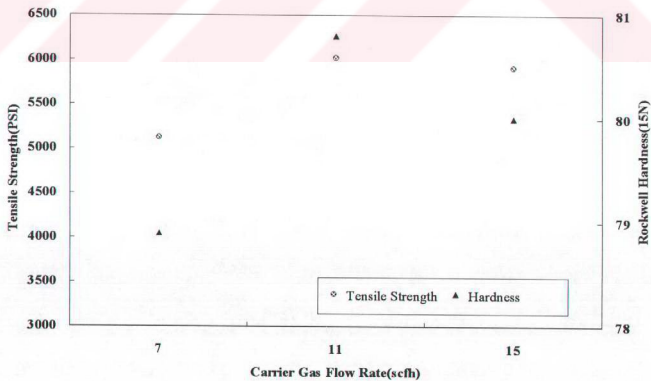


Figure 4.17 Effect of carrier gas flow, at a constant spray rate of 45 gr/min, on the tensile strength and hardness of the coatings.

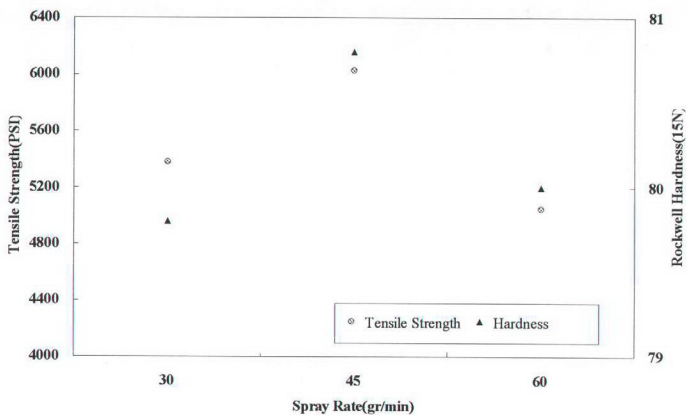


Figure 4.18 Effect of spray rate, at a constant carrier flow of 11 scfh.

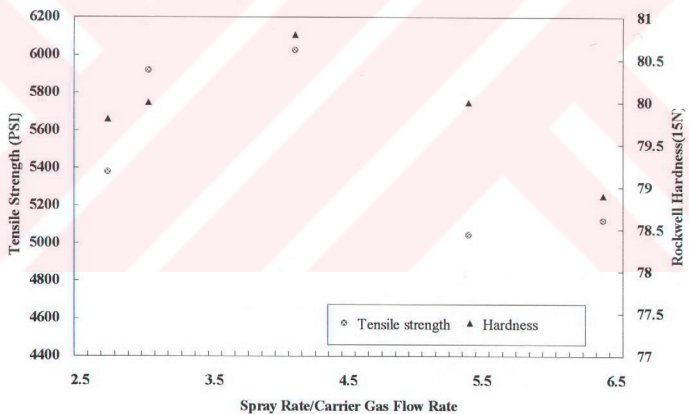


Figure 4.19 Combined effects of spray rate and carrier gas flow, on the tensile strength and hardness of the coatings.

4.1.4 Effect of Preheat

The substrate temperature during deposition is of key importance to the microstructure of the plasma sprayed coatings. It affects the solidification process and thus, also the coating microstructure [24, 27]. The substrate temperature is influenced by many factors like substrate preheating and cooling, gun to substrate distance, plasma energy, and substrate characteristics, [15]. The effect of preheating was determined by changing the number of passes of the plasma flame applied on the coupons before spraying. Of special interest was the deterioration in tensile strength and hardness upon the increasing number of preheat passes (Fig 4.20).

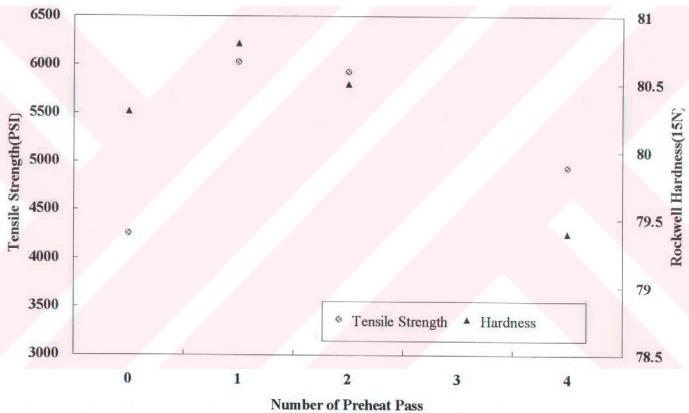


Figure 4.20 Effect of number of preheat passes of the torch on the tensile strength and hardness of the coatings.

The reduction in tensile strength and hardness with increasing preheating may be explained by coarsening of grain structure. However, the microstructure of the coatings prepared with different degree of preheating (Tests 1, 13, 14) showed no significant differences when examined under an optical microscope (Figs 4.4, 4.21, 4.22). Evidently, the resolution obtained by optical microscope is not enough to reveal the grain structure of the coatings.

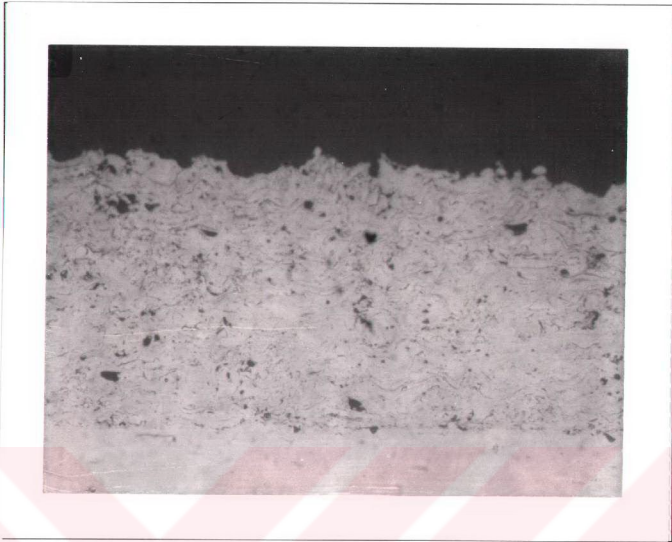


Figure 4.21 Microstructure of the coat, sprayed after two preheating passes (200 \times).



Figure 4.22 Microstructure of the coat, sprayed after four preheating passes (200 \times).

In fact, the strength properties of the coating material are expected to vary with grain size in conformity with the Hall- Petch Equation [10, 28]:

$$S = S_0 + kd^{-1/2} \quad (7)$$

where, S - is the strength of a material (\propto hardness and tensile strength),

S_0 - is the intrinsic strength of a material,

k - is material constant, and

d - is the grain size of a material.

In addition to grain growth, annealing may take place during deposition when the substrate temperatures are sufficiently high. These processes may cause stress relaxation, and coatings with more homogeneous microstructure. Examples of this kind of uniform microstructures may be seen in the Figs 4.21, 4.22.

When preheating is omitted, a lower quality microstructure was produced. A direct comparison of microstructures in Figs 4.4 and 4.23 shows the beneficial effect of preheating.

The degradation of strength properties of coatings under nonpreheated conditions may be attributed to different thermal expansions between substrate and sprayed particles that form additional stresses, and may damage the sprayed layer. Failures such as cracking or layer separation occur when the sprayed coatings cool [18].



Figure 4.23 Microstructure of the coat, sprayed on the nonpreheated test coupon (200 \times).

4.1.5 Effect of Interlayer

The effect of interlayer (bond coat) on hardness was evaluated as a function of spray rate, spray distance and electric input. The reason of using interlayers between the coating and the substrate is, to increase the adherence of the coating with substrate and reduce additional stresses in the coating [19, 20]. The hardness measurements on samples with interlayer gave some results that may be of particular interest (Figs 4.2, 4.23, 4.24):

- 1) Lower hardness values were obtained in the coatings that have interlayers, compared to coatings without the interlayer.
- 2) Examination of fracture surfaces of some tensile specimens showed that separation occurred at the boundary of interlayer with the top coat.

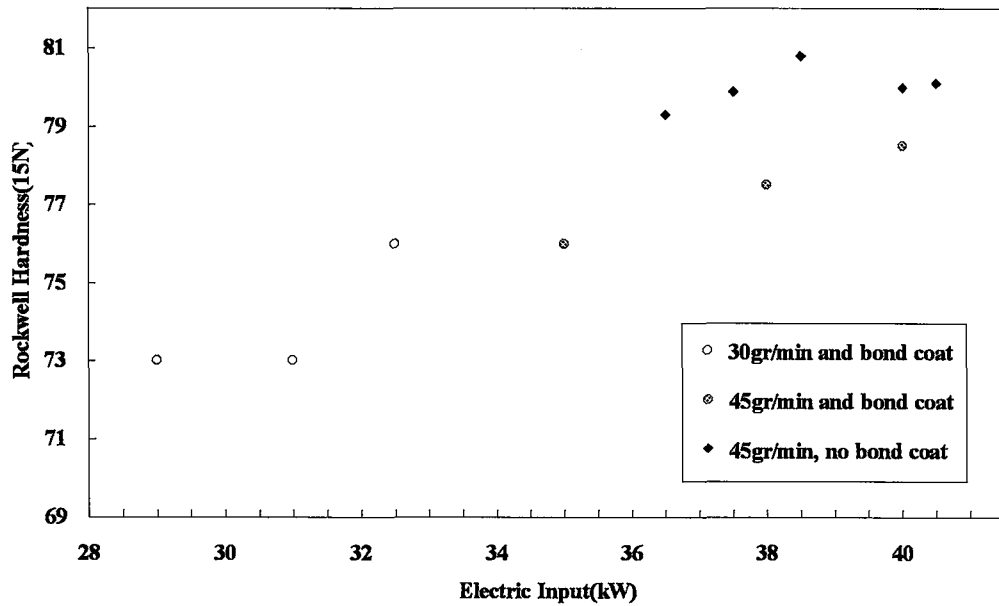


Figure 4.24 Effect of bond coat with different spraying parameters.

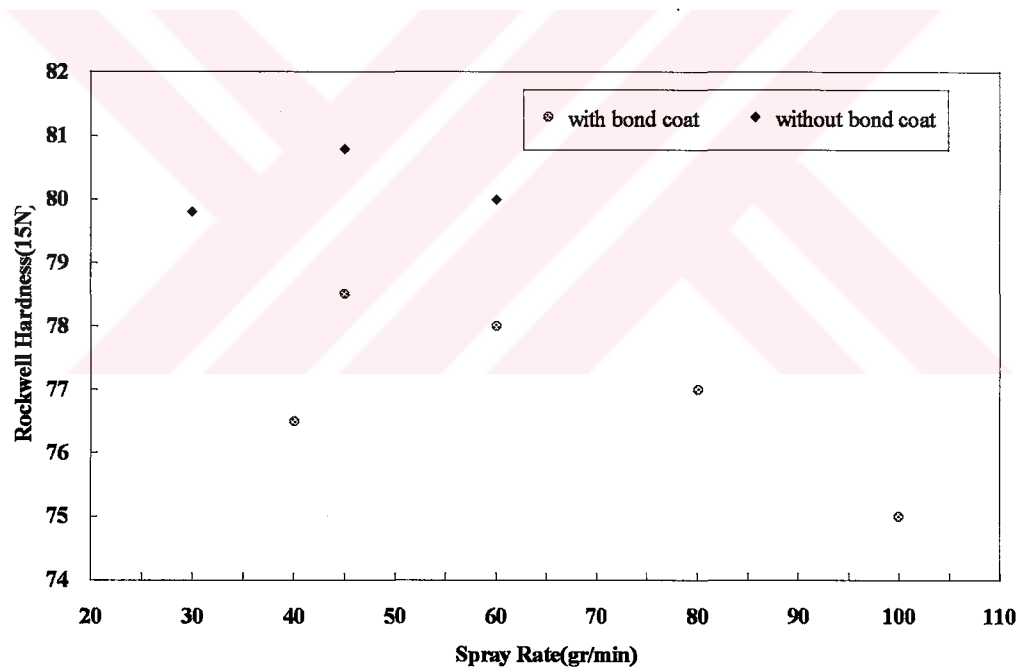


Figure 4.25 Effect of bond coat with different spraying parameters.

The reason of the lower hardness values of these coatings may be due to increasing substrate temperature as a result of longer spraying times. The separation across the interface between bond and top coats was examined by the oxidation of a bond coat during the waiting time before spraying [20, 28]. This oxidation may be

prevented by not making an interruption between bond coat and top coat sprayings, through increasing electric input. Because, higher kinetic energies imparts the effect of this oxide layer and increases cohesive bonding between interlayer and top coat [10].

4.2 Effect of Secondary Plasma Spraying Parameters

The secondary plasma spraying parameters may include traverse speed of spraying on the part, interruption between spraying passes, rotary table speed and air cooling pressure applied on a part during coating. They affect cooling of the part during spraying and also its microstructure, hardness and tensile strength. There are also different types of nozzles that have different orifice diameters. They affect the velocity of the spraying powders. Another indirectly effective parameter is the granularity of the powder. The microstructure of the coating of the same type of powder that was bought from two different suppliers may be different. The reason is, even a small difference in the sizes and shapes of the powders that can not be recognized, before spraying can result in a low quality coating structure. Deteriorating the spraying quality, causes the occurrence of an undesirable microstructure that contains excess amount of voids.

Another secondary parameter is the design of the spraying process. This is very important mostly in the case of spraying of an inside diameter of a part. If the design is not good, air turbulence during spraying can deteriorate the microstructure of the coating.

Spraying angle is equally important. After several sprayings of a part, it was found the worsening the microstructure and poor adhesion and delamination of the coatings, if the angle is decreased from 90° to 45° [29]. However, 90° angle may not be always possible due to the complex shape of the part. This time, the nearest angle to 90° should be used.

A study, to observe and eliminate the negative effects of some of these indirectly effective parameters, was done on an aircraft engine part of TEI (Tusas Engine Industries). After the occurrence of suddenly unexplained deterioration on the

microstructure of the part coat, the problem was solved after a systematic approach of the special process department of TEI. The procedure to obtain the satisfactory results are summarized in the flowchart in Appendix.

From this flowchart the following positive effects on the coating quality can be deduced:

- a) increasing the traverse speed of the plasma torch and the turn table speed, results in cooling of substrate during spraying,
- b) decreasing the hole diameter of the nozzle, increases the powder velocity, resulting in denser coating,
- c) improved part fixture design to prevent air turbulence during spraying. can prevent the coating structure against deterioration.



CHAPTER 5

CONCLUSIONS

- 1) Increasing electric input, through increasing plasma gas volume, improves tensile strength, hardness. However, the further increase of plasma gas volume causes cooling effect, resulting in deterioration in the density of the coating accompanied with a reduction in strength properties.
- 2) At shorter spraying distances, the plasma beam hits the substrate and overheats it considerably, causing exceedingly molten particles to splash, creating a less dense structure. At larger distances, due to an oxidation effect, deterioration of the coating microstructure and other properties are observed.
- 3) Spray rate and carrier gas flow rate are other primary parameters, that should be adjusted cooperatively, in order to obtain a sound microstructure of the coatings.
- 4) Increasing preheating times of the substrate increases coating temperature. Therefore, the tensile strength and hardness values decrease due to annealing of coating material. In the case of nonpreheated substrate however, thermal stresses may weaken all mechanical properties.
- 5) Existence of an interlayer (bond coat) causes effects on the properties of the coatings, similar to those of preheating. Furthermore, oxidation that occurs on the interlayer before spraying the top coat deteriorates the tensile strength.
- 6) In addition to primary parameters, there are also some secondary factors that should be investigated systematically. By the help of more advanced techniques;

like SEM, TEM or X-Ray Diffraction, it can be easier to analyze the effects of above parameters on the microstructure of the coatings. Although, in many cases, these parameters are ignored, their effects can be tremendous. Furthermore, both primary and secondary parameters can be converted to fundamental plasma parameters to make standardization in this process.



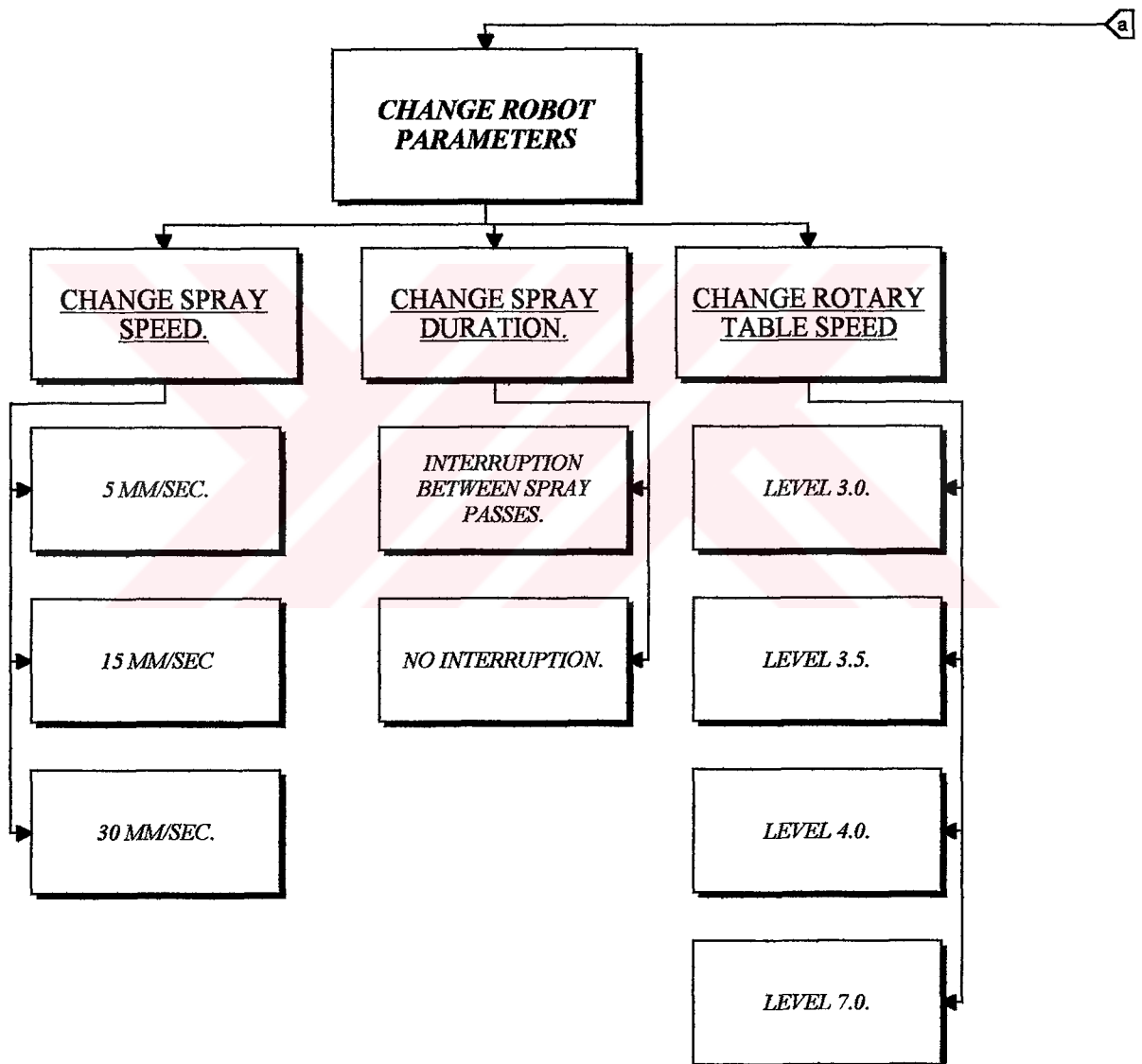
REFERENCES

- [1] Plasmatechnik AG, Technical bulletins, Wohlen (1994)
- [2] Metco, Technical bulletins, Wetsbury (1994)
- [3] Progressive Technologies, Technical Bulletins, USA (1994)
- [4] Unpublished Data, İhsan Güler (1994)
- [5] General Electric, Technical Bulletins, USA (1994)
- [6] D. Matejka, B. Benko, Plasma Spraying of Metallic and Ceramic Materials, (1989)
- [7] Anderson, J.C., Proc. Int. Conf., Advances in Surface Coating Technology, The Welding Institute, Cambridge, United Kingdom, (1978)
- [8] P. Meyer and S. Muehlberger, Thin Solid Films, ,445, 456 (1984)
- [9] D.Apelian, D. Wei and M. Paliwal, Thin Solid Films, ,395, 407 (1984)
- [10] S. Safai, H. Herman, Thin Solid Films, ,295, 307 (1977)
- [11] H. Eschnauer, Thin Solid Films, 1, 17 (1980)
- [12] S. Dallaire and B. Champagne, Thin Solid Films, 477, 483 (1984)
- [13] R. McPherson, Thin Solid Films, 297, 310 (1981)
- [14] D. Chuanxian, R.A. Zatorski, H. Herman and D. Ott, Thin Solid Films, 467, 475 (1984)
- [15] B. Gudmundsson, B. E. Jacopson and H. Gruner, Materials Science and Engineering, 105, 115 (1989)
- [16] W. Wilms and H. Herman, Thin Solid Films, 251, 262 (1976)
- [17] P.F.Becher, R.W.Rice, C.C.Wu and R.L.Jones, Thin Solid Films, 225, 232 (1978)
- [18] C.C. Li, Thin Solid Films, 59, 77 (1980)
- [19] S. Kuroda and T.W.Clyne, Thin Solid Films, 55, 66 (1990)

- [20] W. Lih, E. Chang, B.C. Wu and C.H. Chao, Oxidation of Metals, Vol. 36, Nos. 3/4, (1991)
- [21] General Electric, GEAE Specifications, USA (1994)
- [22] Standard Test Methods for Rockwell Hardness and Rockwell Superficial Hardness of Metallic Material, ASTM E 18 (1986)
- [23] H.Kayzer, Thin Solid Films, 243, 250 (1976)
- [24] S.J. Harris and M.P. Overs, Thin Solid Films, 495, 505 (1984)
- [25] H.Gruner, Thin Solid Films, 409, 420 (1984)
- [26] J. Hennaut, J. Othmezzouri and J. Charlier, Thin Solid Films, 97, 109 (1990)
- [27] S. Dallaire, Thin Solid Films, 237, 244 (1982)
- [28] D. R. Mash, I. M. Brown, Metals Eng. Q., 18, 32 (1964)
- [29] Tusaş Engine Industries, Technical bulletins, Turkey (1994)

APPENDIX

TEST PROCEDURE TO IMPROVE THE COATING QUALITY OF AN AIRCRAFT ENGINE PART OF TEI



**PARAMETERS THAT
CAN BE CHANGED TO
CATCH AN
ACCEPTABLE
MICROSTRUCTURE**

**CHANGE PLASMA
PARAMETERS.**

**CHANGE POWER
INPUT.**

37.5 kW.

39.0 kW.

42.9 kW.

**CHANGE SPRAY
ANGLE.**

WITH 45.

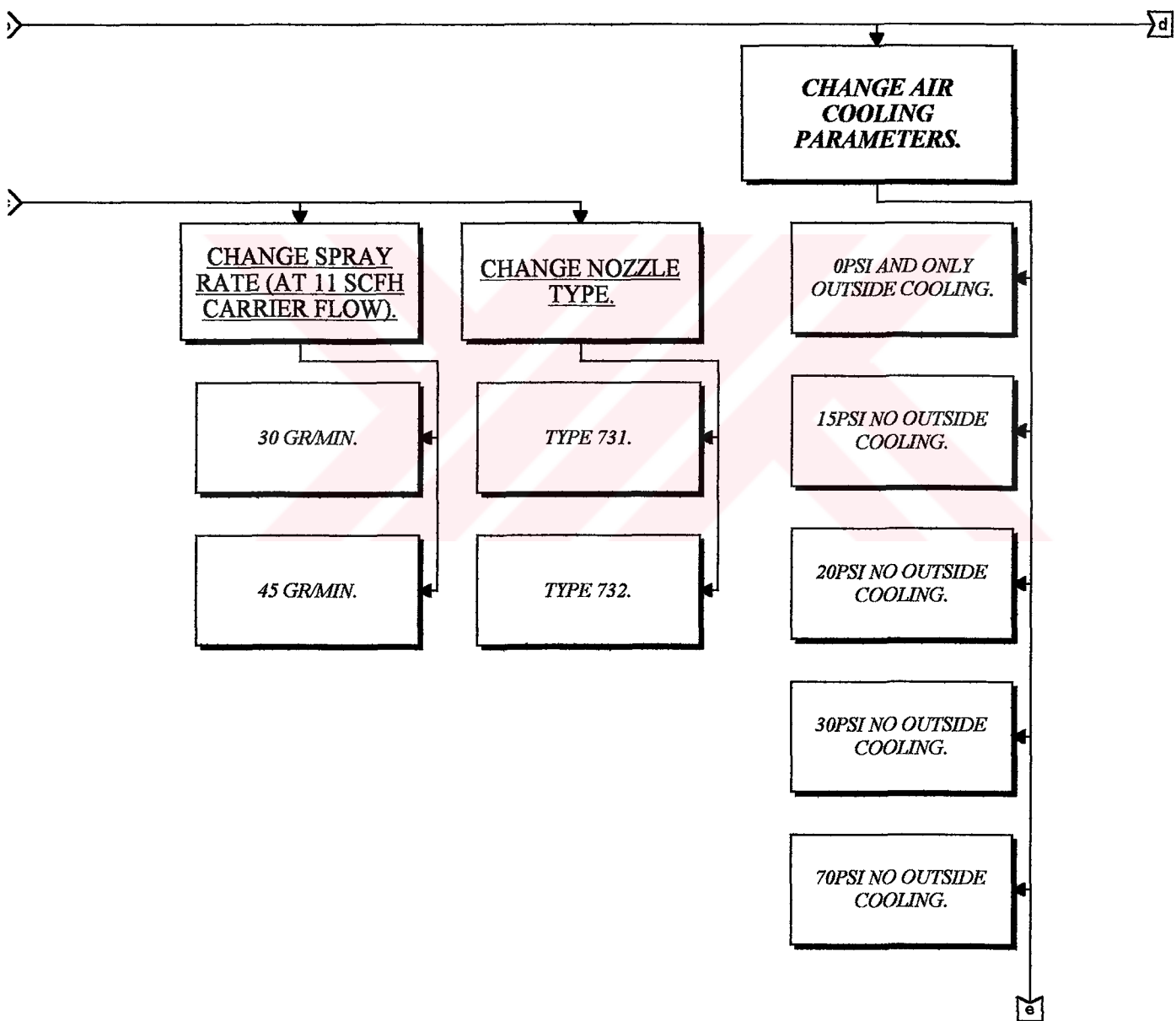
WITH 50.

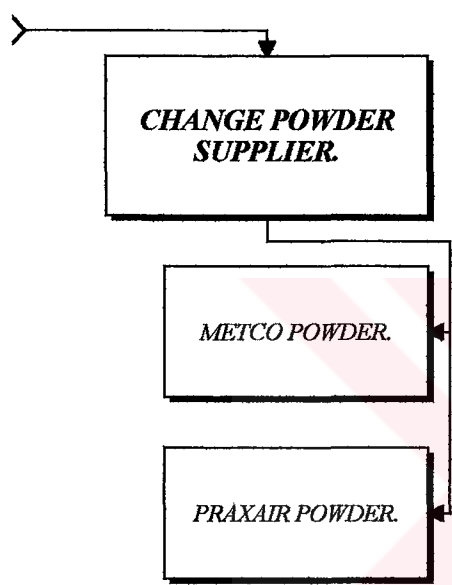
**CHANGE SPRAY
DISTANCE.**

WITH 3.5".

WITH 4".

WITH 5.5".





e

80PSI NO OUTSIDE
COOLING.

CHANGE THE FIXTURE
DESIGN TO PREVENT
AIR TURBULANCE.

CHANGE ROTARY
TABLE ANGLE TO
PREVENT AIR
TURBULANCE.

T.C. YÜKSEKÖĞRETİM KURULU
DOKÜMANTASYON MERKEZİ